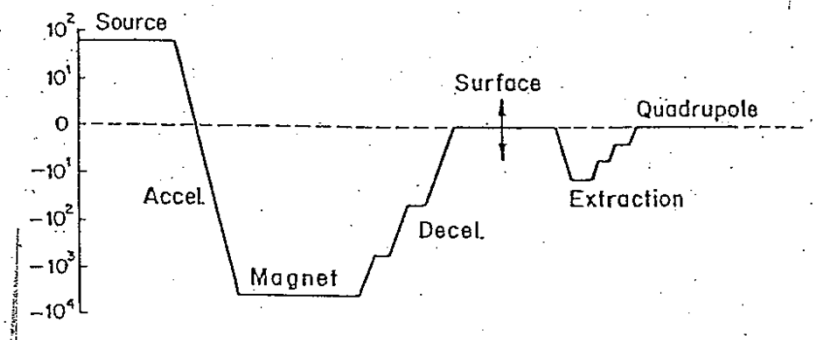


MS Short Course at Tsinghua  
Lecture 8 – 9  
Mass Analyzer and MS Instrumentation

# Ion Optics

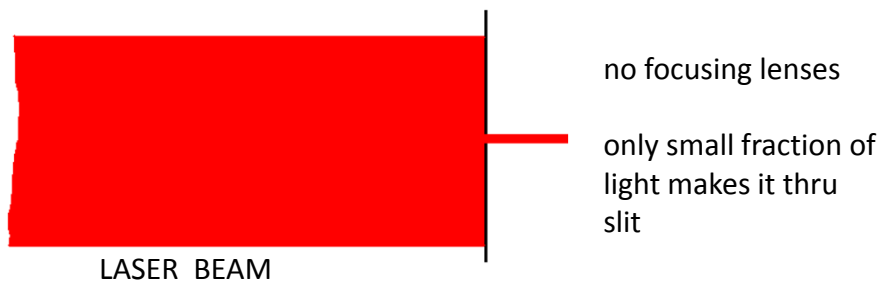
## 1. Potential along ion optical axis



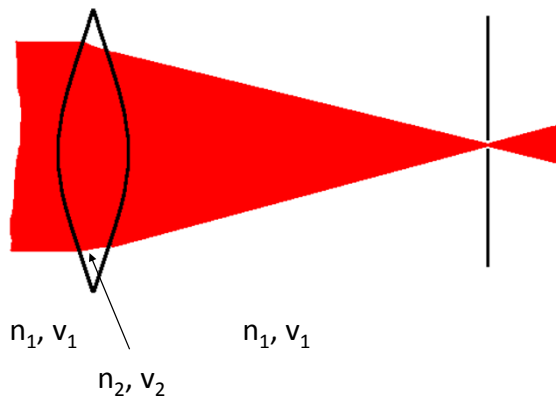
## 2. Comparison with light optics

Same objective

Shine laser onto small slit:

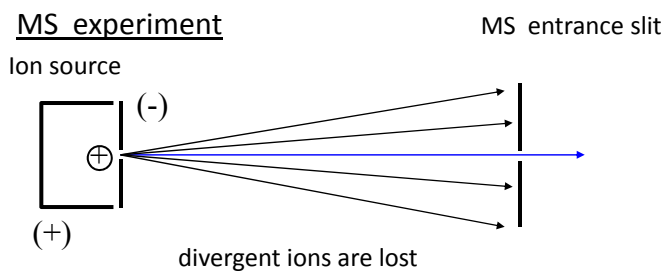


Use lens to focus beam into slit



velocity of beam changes inside lens

lens surface curved  $\Rightarrow$   
off-axis rays are deflected and focused



Insert lens between source and slit

collimate divergent ions thru slit

improve transmission and sensitivity

set of metal lenses: circular apertures or cylinders

apply DC voltages to focus

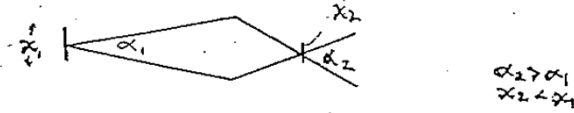
<u>Objective</u>	<u>Optical Lens</u>	<u>Ion Lens</u>
CHANGE VELOCITY	pass beam into medium of different density	pass beam thru region of different E field
DEFLECT BEAM	curve/tilt boundary of different media	curve/tilt potential contours

**Conservation Theorem: Liouville's Theorem**

Product  $x \cdot \alpha \cdot v = \text{constant}$ ,  $x$  dimension,  $\alpha$  angle and  $v$  velocity

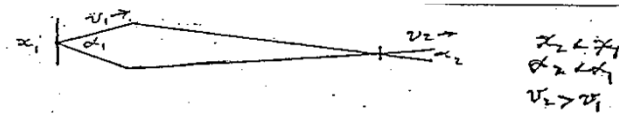
At constant velocity phase space  $x, \alpha$  is constant, can only reduce size of image by increasing angle.

Acceleration is easiest way to focus (but many expts don't allow!)



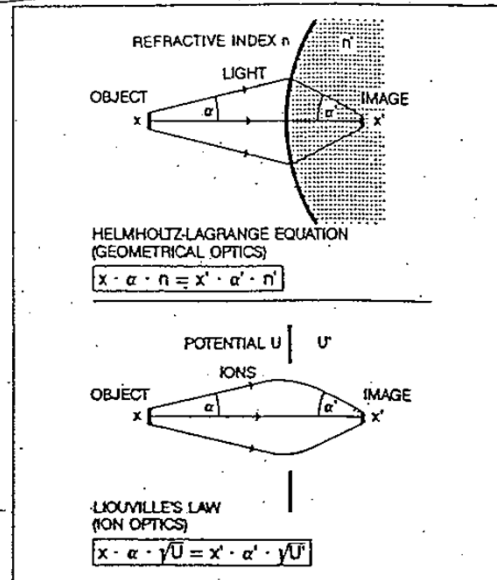
If one focuses without change in energy it is necessarily done at expense of angular divergence [which means any error in position of image is magnified in image size]

One can get good focusing ( $x_2 < x_1$ ) without angular divergence only by acceleration beam:



Post acceleration is part of high quality ion optics but it simply hides errors--the quality of the pre-accelerated beam the essential matter.

**Helmholtz-Lagrange equation and Liouville's theorem**



### 3. Electrostatic weak lenses

Field penetration produces curvature in equipotential lines, this second order effect is used for focusing: [fringe fields]

Immersion lens (two sections w. difference in potentials and hence velocities) not good for focusing. —necessarily change KE

Electrostatic lenses are always convergent, never divergent as light, optic lenses often are. To get divergence in an optical lens one uses a “cross—over” which means one focuses the beam to a point, after which the trajectories diverge. The small spot on a tube is an image of a cross-over made near the cathode of the electrode gun.

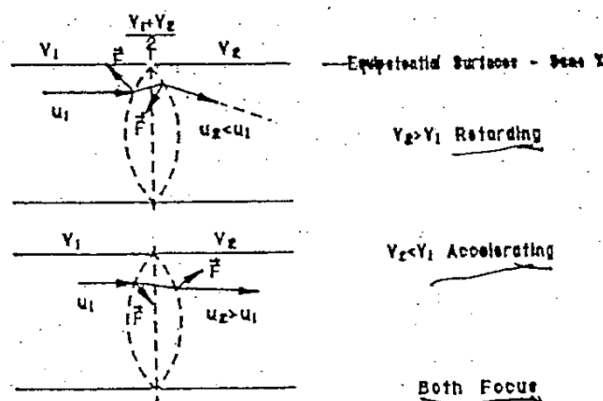


Fig. 11A

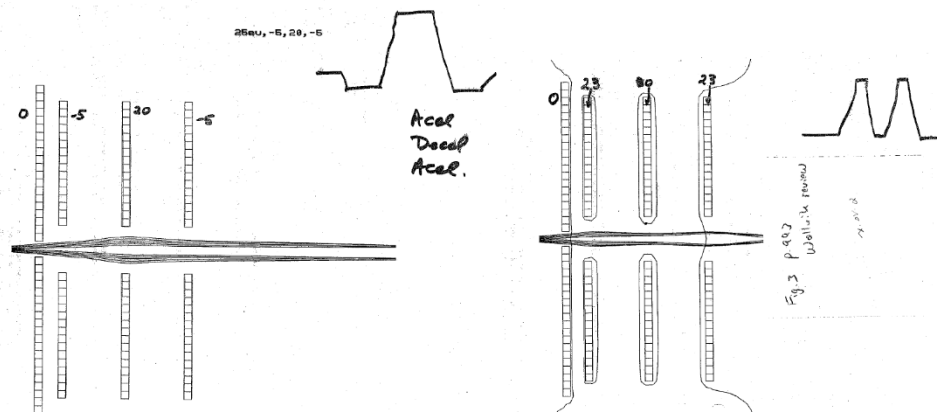
**Thin Lens: Einzel lenses**

Einzel = single

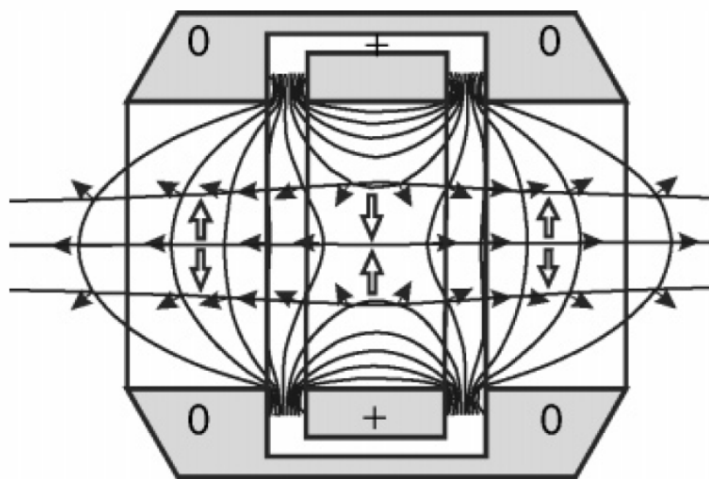
Good lens for focusing requires three lens elements this gives two lens element intersections which can be accel -- decel -- accel OR decel -- accel -- decel

So even w/o changing overall energy of the beam there are strong potential changes which form the basis for the forces at right angles to beam direction which are basis for focusing.

As usual, there is no force on beam along ion optical axis.

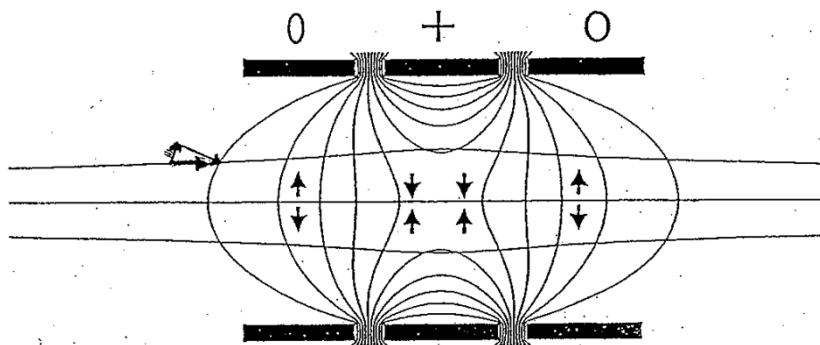


**Thick Lens**



Convergence

Electrostatic lens intersections are always convergent (unlike light optics) forces are always towards the ion optical axis

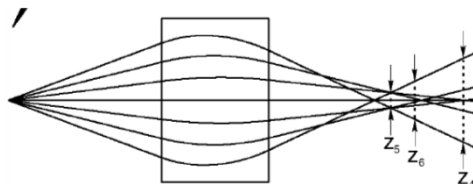


4. Aberrations in Ion Optics

Spherical- ions farther from axis cross at different pts than those near axis center (field strength)

Solution:

- skim off outer part of beam (lose ions)
- keep lens diameter  $\gg$  ion beam size

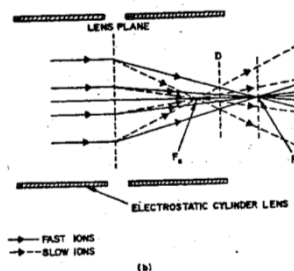


H. Wollnik, J. Mass Spectrom., 34, 991-1006 (1999).

Chromatic- ions with different KE have different focal pts

Solution:

- brute force (keep  $KE/\Delta KE$  large)



Thick and thin lenses

As stated.

Thin need higher potentials, might need surrounding potential defining screen, but use distance more effectively, allow pumping, etc

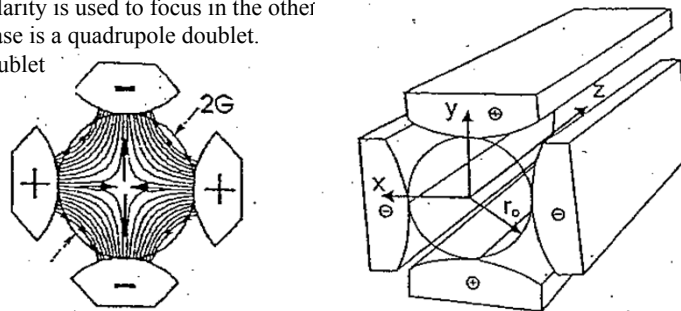
5. Strong focusing

Weak focusing uses forces due to second order (fringe or lens element intersection) effects with no force in radial direction except due to fringe effects; strong focusing uses lens elements with radial forces directly proportional to distance from axis or higher.

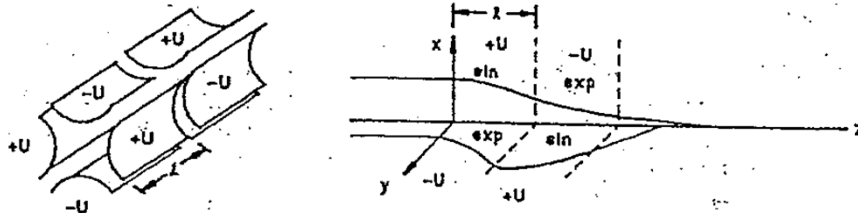
These forces will be focusing in one direction but will disperse in the other so a second lenses with opposite polarity is used to focus in the other  
 Most common case is a quadrupole doublet.

DC: 1 quad of doublet

RF: 1 quad only



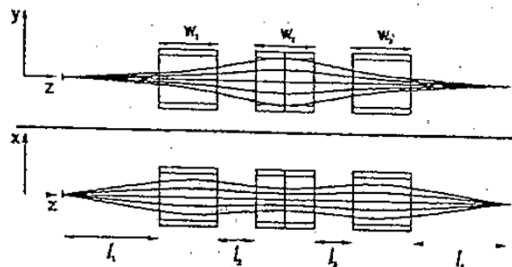
Combination of DC quadrupole provide flexibility in shaping/focusing the beam



This example illustrates a quad pair that leads to astigmatic focusing (focal points for x and y are not coincident on z)

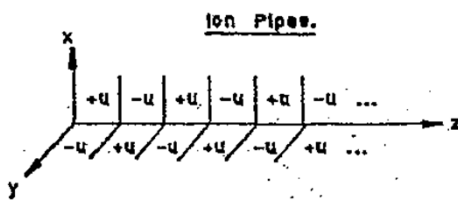
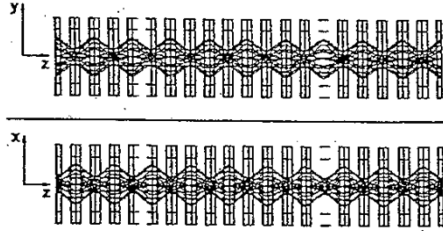
3-element quad lens system with stigmatic focus

Figure 9 A quadrupole triplet that achieves stigmatic focusing ( $x/a = (y/b) = 0$  and a 1:1 magnification in both the x and y-directions, i.e.  $(x/x)(y/y) = -1$ . Note that the ion trajectories, that diverge from one point initially, are all parallel in the middle of the quadrupole triplet at which position the x, y beam envelopes differ considerably.

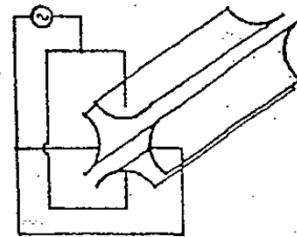




An ion pipe



Equivalent to



Stable trajectories if  $\frac{m}{e} \geq \frac{2u}{(3.75)^{1/2} \lambda}$

- All multipoles consist of 2n symmetrically arranged elements
- n=2 quadrupole
- 3 hexapole
- 4 octapole
- 5 decapole
- 6 dodecapole

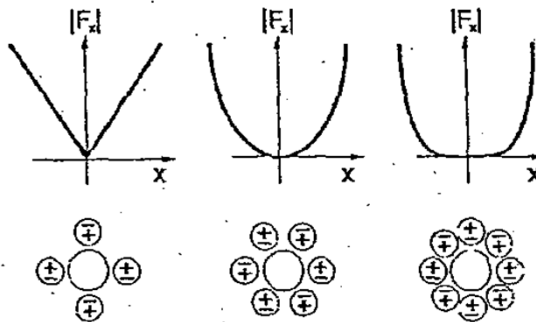
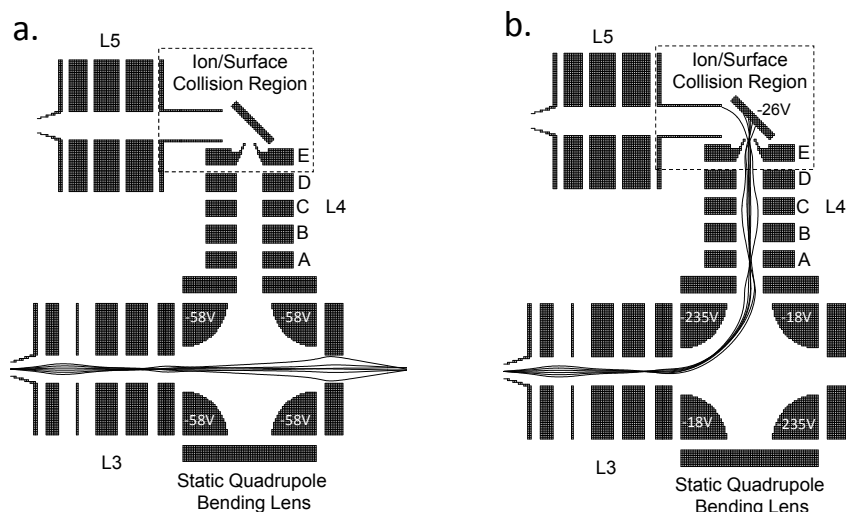


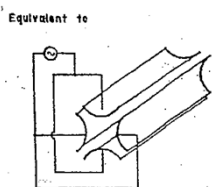
Figure 20. The absolute values of the back-driving forces  $F$  in the  $x$ -direction that ions experience in an electric quadrupole ( $2n=4$ ), hexapole ( $2n = 6$ ) or octupole ( $2n= 8$ ) are plotted as a function of the distance  $r$  from the optical axis.  
 All multipole devices exhibit a high pass filtering action

Static Bending lens

1. initialize ion beams with certain m/z, KE and dispersion angle, etc.
2. Use Einzel lens set 1 to focus the ion beam
3. Use reflection quadrupole electrodes to bend the ion beam by 90°
4. Use Einzel Lens set to focus the bent ion beam to get maximum output.



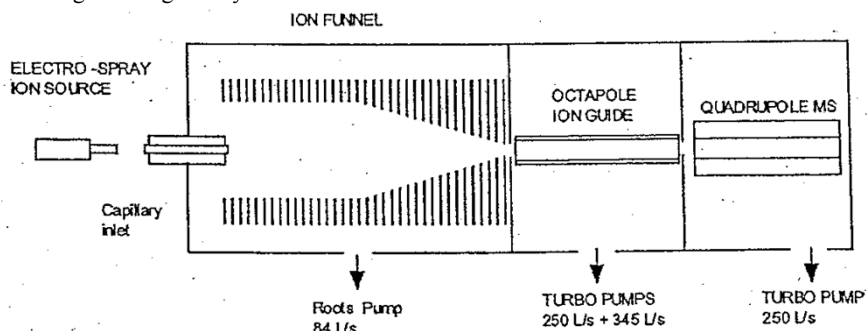
6. Electrical Dynamic Lens:



Stable trajectories if  $\frac{m}{q} \geq \frac{8V}{(3.75)kV}$

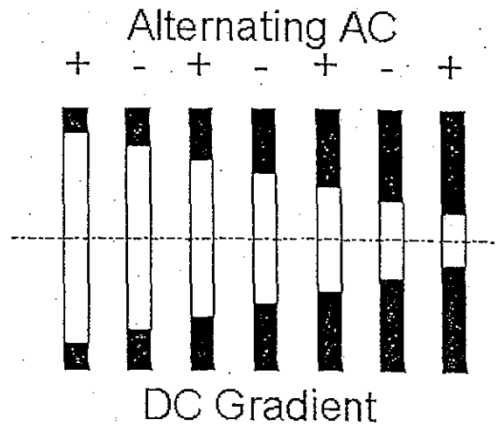
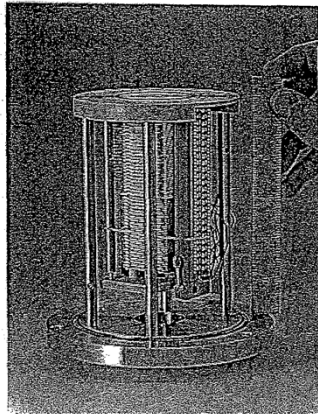
Ion funnel

Deceleration, especially by large factor without decoupling is difficult; deal with strong focusing is very hard. Solution is the ion funnel.

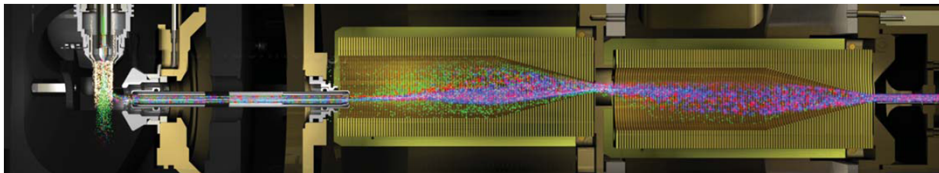


Schematic diagram of the ion funnel interface in the context of the overall instrumentation

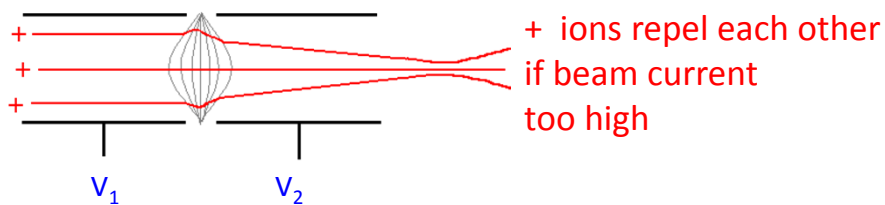
PNNL



Agilent iFunnel



7. Space Charge- limits minimum beam diameter



$$Force = \frac{eI_0}{2\pi\epsilon_0vr} = eE_r$$

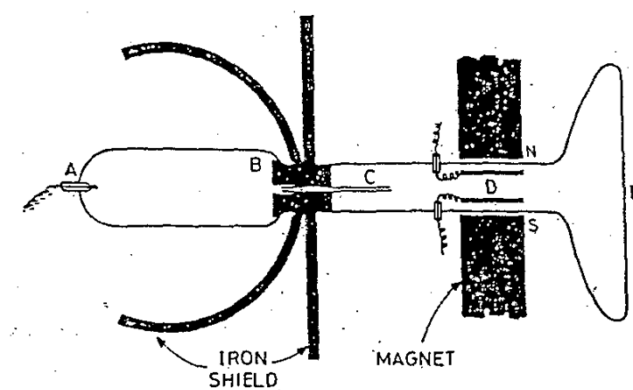
assume beam is  
 cylindrical

Space charge increases with:

- ↑  $I_0$
- ↓  $v$
- ↓  $r$

## Mass Analyzers

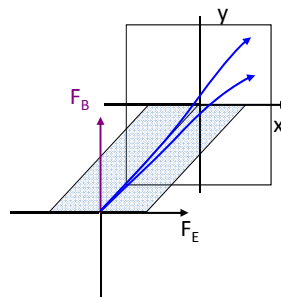
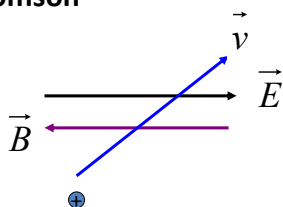
### Thomson' apparatus



C. Capillary  
B. Cathode  
A. Al anode 20 kV  
E. Detection (willenite) fluorescence o photoplate  
Vacuum using rotary pump  
Parallel B, E fields

$$\vec{F} = q(\vec{E} + \vec{v} \times \vec{B})$$

Thomson



Wien

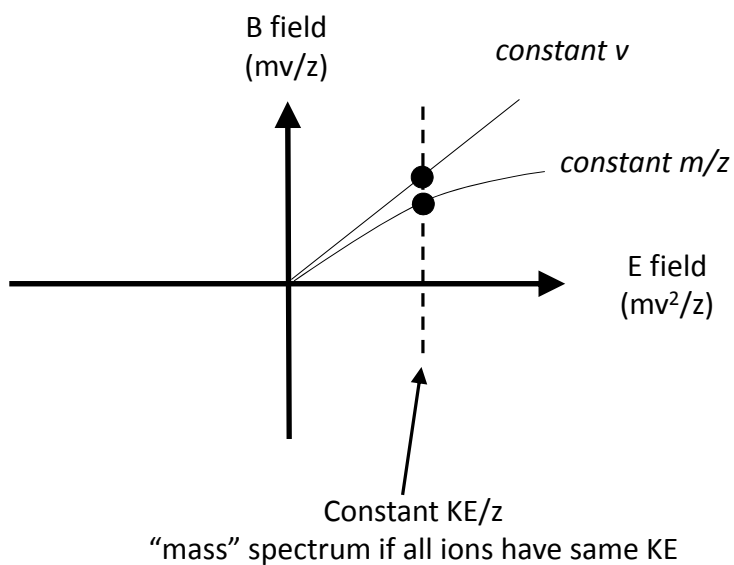
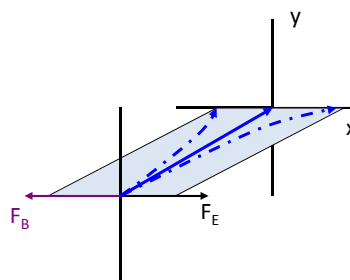
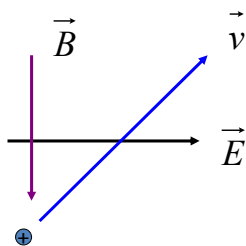
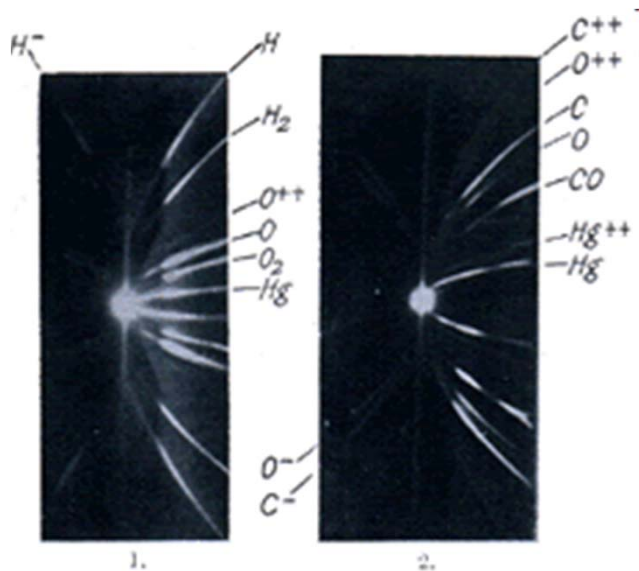


Photo of Thomson's data



<http://www.phy.cam.ac.uk/camphy/index.htm>

#### Mass Analysis and Mass Analyzers

- The mass of a molecule cannot be directly weighed.
- The  $m/z$  value of an ion cannot be directly measured.
- Mass analysis is a gas phase separation of the charged particles.
- Separation in space –trajectory based MS analyzers
  - Sectors
  - Time of Flight
- Separation in motion frequency –Trap type MS analyzers
  - Quadrupole filter/ion trap
  - Ion cyclotron resonance (ICR)
  - Orbi-trap

### Characteristics of Mass Analyzers

Method	Quantity measured	Mass/Charge range (Da/charge)	Resolution at 1000 (Da/charge)	Mass Accuracy at 1000 Da/charge	Dynamic range <sup>b</sup>	Operating Pressure (Torr)
Sector Magnet	Momentum / charge	10 <sup>4</sup>	10 <sup>5</sup>	<5 ppm	10 <sup>7</sup>	10 <sup>-6</sup>
Time of flight	flight time	10 <sup>6</sup>	10 <sup>3</sup>	0.01%	10 <sup>4</sup>	10 <sup>-6</sup>
Quadrupole ion trap	frequency	10 <sup>4</sup> -10 <sup>5</sup>	10 <sup>3</sup> -10 <sup>4</sup>	0.1%	10 <sup>4</sup>	10 <sup>-3</sup>
Quadrupole	filters for m/z	10 <sup>3</sup> -10 <sup>4</sup>	10 <sup>3</sup>	0.1%	10 <sup>5</sup>	10 <sup>-5</sup>
Cyclotron resonance	frequency	10 <sup>5</sup>	10 <sup>6</sup>	<10 ppm	10 <sup>4</sup>	10 <sup>-9</sup>
Orbi Trap	Frequency	10 <sup>5</sup>	10 <sup>6</sup>	<10 ppm	10 <sup>4</sup>	10 <sup>-9</sup>

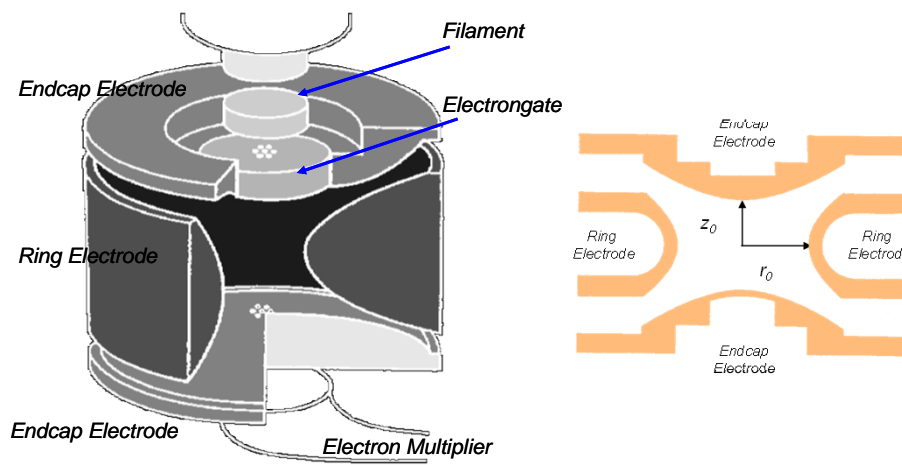
<sup>a</sup>Mass/peak width

<sup>b</sup>Number of orders of magnitude of concentration over which response varies linearly.

### Quadrupole MS Filter and Quadrupole Ion Trap

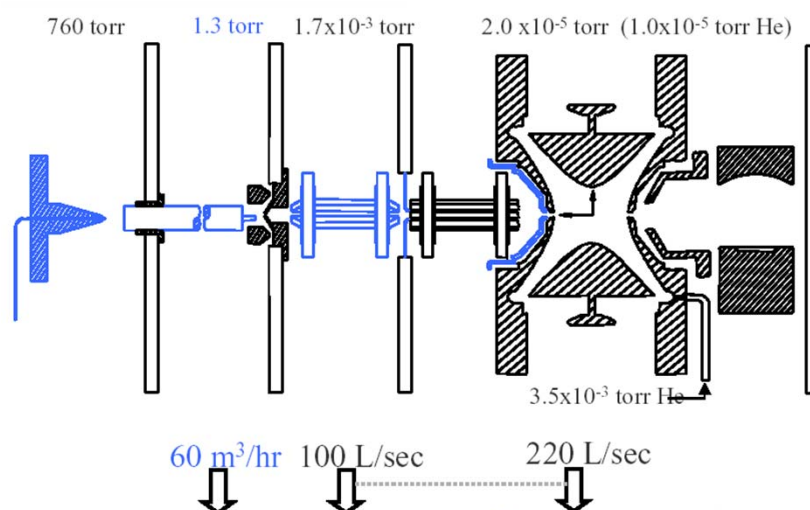
### 1. Geometry of MS analyzer and Instrument Configurations

#### Geometry of ion trap/ internal EI



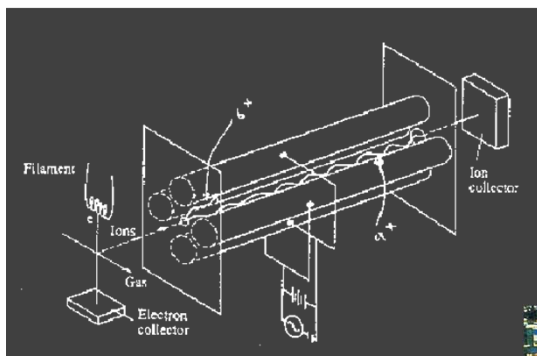
#### Instrument with atmospheric pressure ionization

#### Operating pressures and optics





## Quadrupole Mass Spectrometer



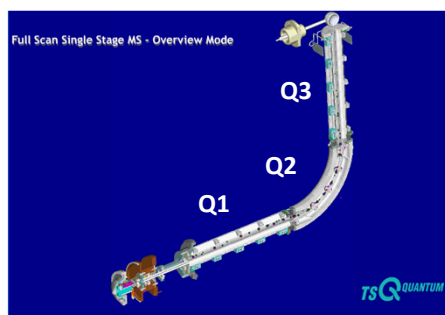
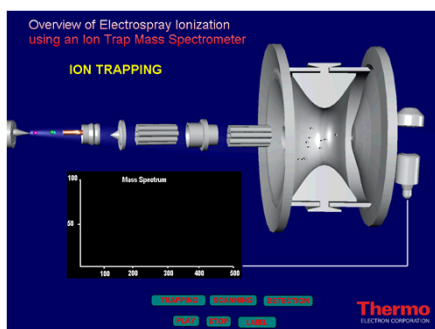
Finnigan

## Quadrupole Mass Spectrometer



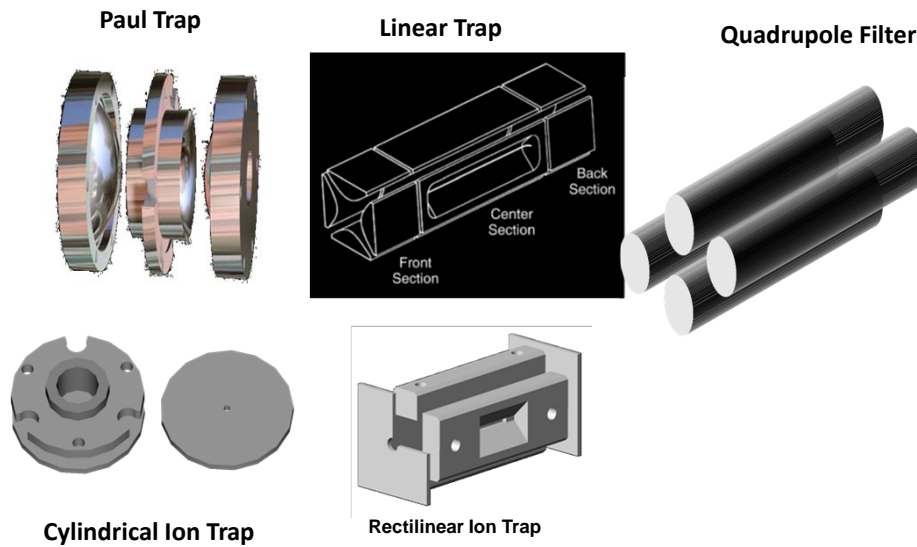
Valley of the Drums  
Superfund Site

<http://www.chm.bris.ac.uk/~paulmay/misc/msc/msc3.htm>



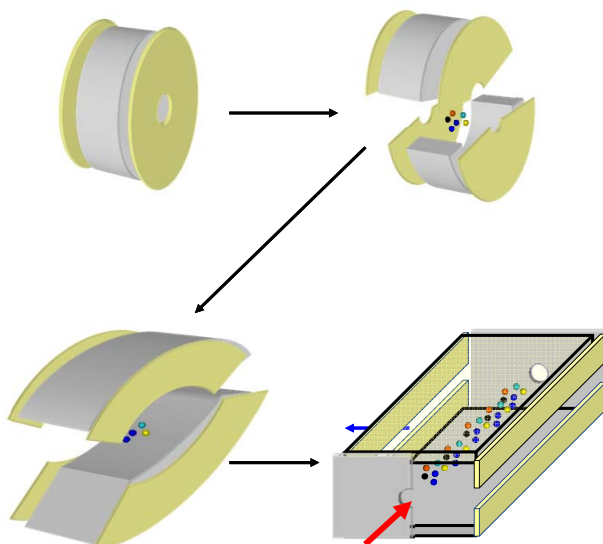
### 3D vs. Linear

---



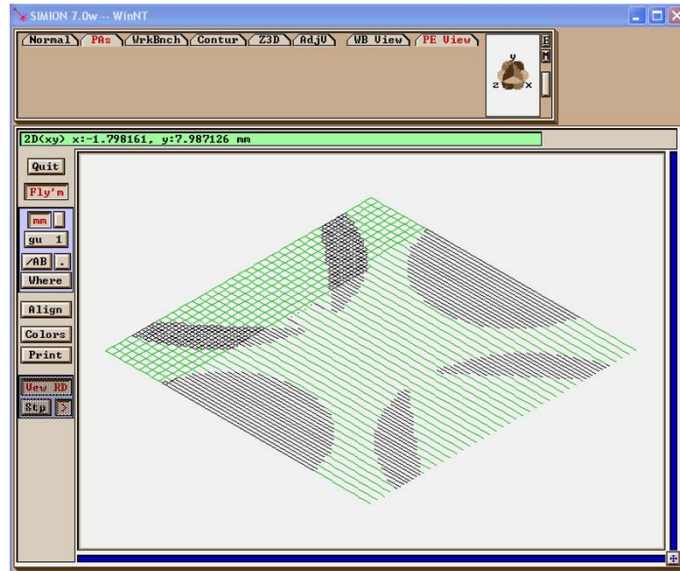
### 3D vs Linear

---

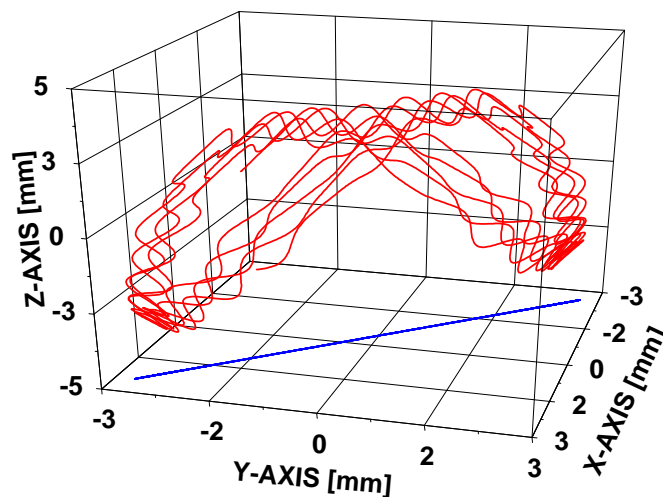


## 2. Theory

SIMION Simulation of Ion Trap RF Field



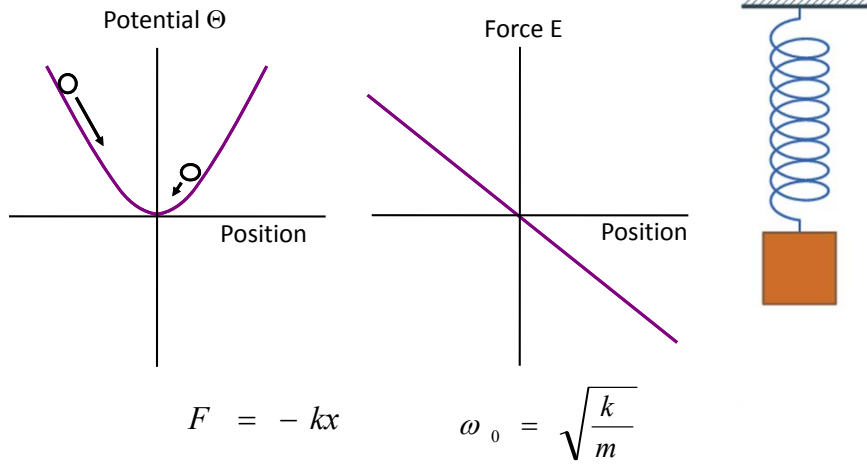
## Ion Trajectory



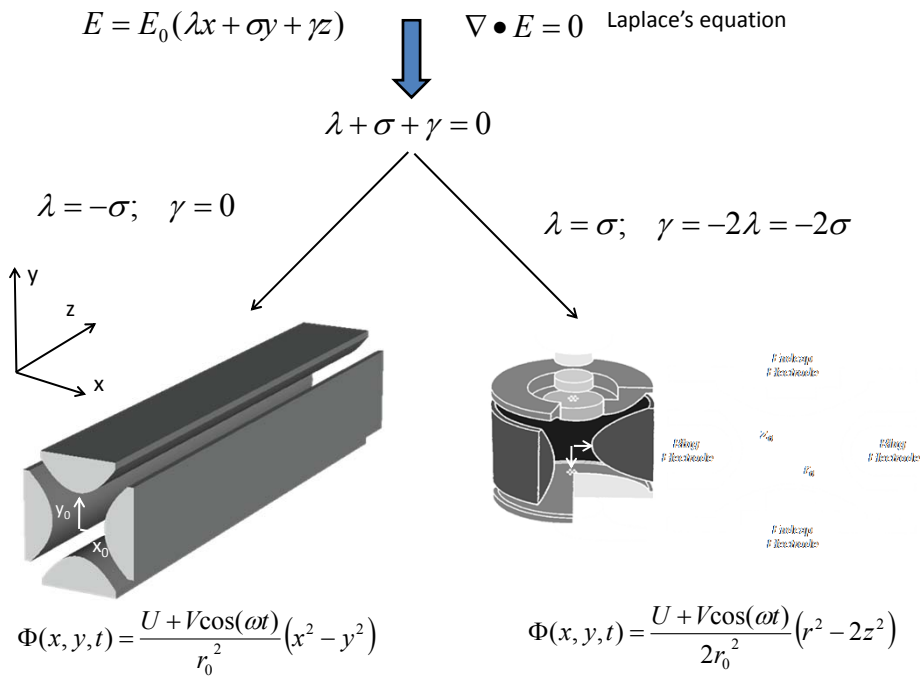
Ion Trap RF Field

Quadrupolar Field

Harmonic oscillator



Circular frequency is INDEPENDENT on the KE and Position of the ion.



Quadrupole filter

$$\Phi(x, y, t) = \frac{U + V \cos(\omega t)}{r_0^2} (x^2 - y^2)$$

3D Trap

$$\Phi(x, y, t) = \frac{U + V \cos(\omega t)}{2r_0^2} (r^2 - 2z^2)$$

$$m \frac{d^2 u}{dt^2} = ma = F = eE_u = e \frac{d\Phi}{du}$$

$$\frac{d^2 x}{dt^2} + \frac{e}{mr_0^2} (U - V \cos(\omega t)) x = 0$$

$$\frac{d^2 z}{dt^2} - \frac{2e}{mr_0^2} (U - V \cos(\omega t)) z = 0$$

$$\frac{d^2 y}{dt^2} - \frac{e}{mr_0^2} (U - V \cos(\omega t)) y = 0$$

$$\frac{d^2 r}{dt^2} + \frac{e}{mr_0^2} (U - V \cos(\omega t)) r = 0$$

$$a_u = a_x = -a_y = \frac{4eU}{mr_0^2 \Omega^2}$$

$$a_z = -2a_r = -\frac{8eU}{mr_0^2 \Omega^2} = -\frac{4eU}{mz_0^2 \Omega^2}$$

$$q_u = q_x = -q_y = \frac{2eV}{mr_0^2 \Omega^2}$$

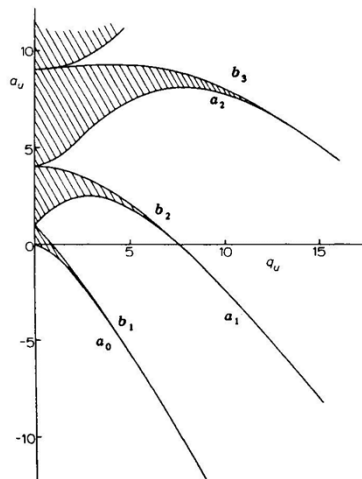
$$q_z = -2q_r = -\frac{4eV}{mr_0^2 \Omega^2} = -\frac{2eV}{mz_0^2 \Omega^2}$$

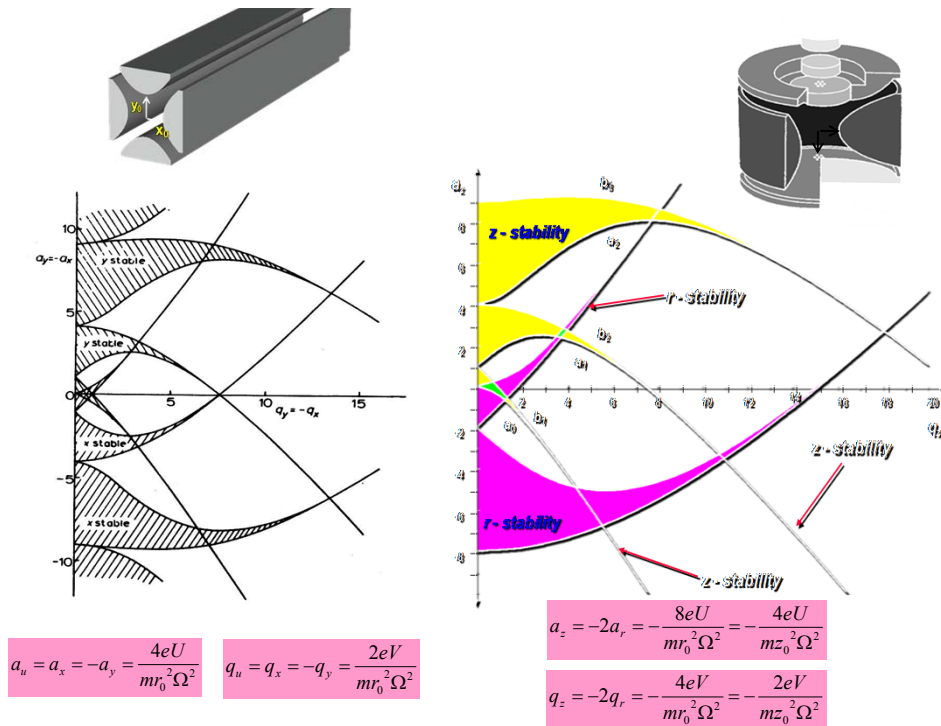
Mathieu equation

$$\frac{d^2 u}{d\xi^2} + (a_u - 2q_u \cos(2\xi)) u = 0 \quad \xi \equiv \frac{\Omega t}{2}$$

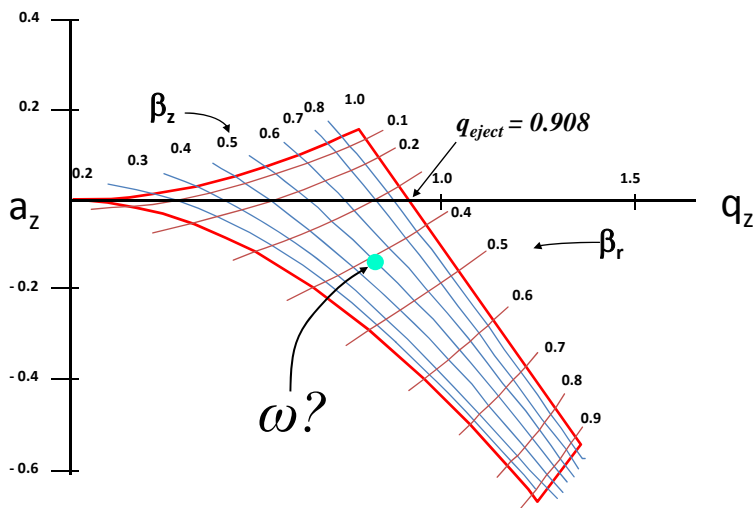
41

$$\xi \equiv \frac{\Omega t}{2}$$





Mathieu Stability Diagram



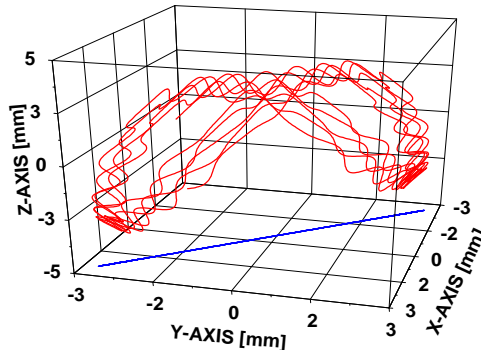
$$\beta_u^2 = a_u + \frac{q_u}{(\beta_u + 2)^2 - a_u - \frac{q_u^2}{(\beta_u + 4)^2 - a_u - \frac{q_u^2}{(\beta_u + 6)^2 - a_u - \dots}}$$

$$+ \frac{q_u}{(\beta_u - 2)^2 - a_u - \frac{q_u^2}{(\beta_u - 4)^2 - a_u - \frac{q_u^2}{(\beta_u - 6)^2 - a_u - \dots}}$$

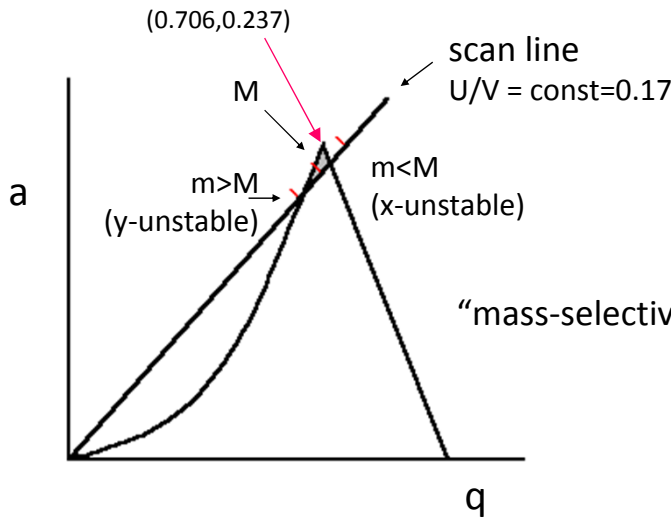
$$\beta_u \cong \sqrt{a_u + q_u^2 / 2}$$

(for  $q_u < 0.4$ )

$$\omega_{n,u} = (2n \pm \beta_u) \frac{\Omega}{2}$$



3. RF and DC operation: Mass filter

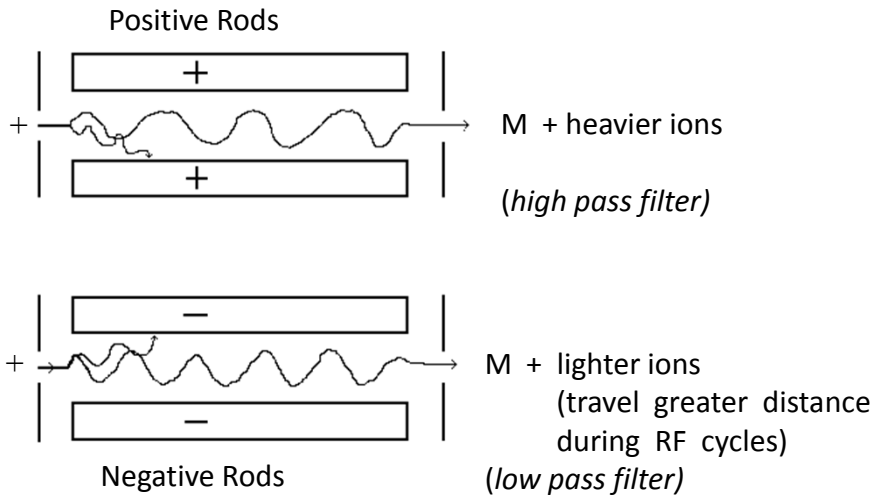


$$a_u = \frac{4zeU}{mr_0^2 \Omega^2}$$

$$q_u = \frac{2zeV}{mr_0^2 \Omega^2}$$

\*scan electronically, change stable m/z (1000 Th/s)

Filtering action



RF: light ions follow and are made unstable (when RF>DC) = high pass  
 DC: heavy ions made unstable (inertia) = low pass

47

Mass Filter - Mass range

$$q_{\max} = \frac{4zeV_{\max}}{mr_0^2\Omega^2} = 0.706$$

$$\left(\frac{m}{z}\right)_{\max} = \frac{4eV_{\max}}{(0.706)r_0^2\Omega^2}$$

- Increase V- practical limits
- Decrease  $r_0$ - practical limits
- Decrease  $\Omega$ - easy, but affects resolution

$$\left(\frac{m}{\Delta m}\right) \propto (\#cycles)^2$$

increase length, but then have mechanical limits

48



Quad calcs:

1) time of flight: m/z 100; 10 eV (= 1.602x10<sup>-18</sup> J); L=20 cm

$$E=0.5mv^2=0.5m(d/t)^2$$

$$t = d \sqrt{\frac{m}{2E}} = (0.2) \sqrt{\frac{1.66 \times 10^{-25}}{2 * 1.602 \times 10^{-18}}} = 45 \text{ } \mu\text{s}$$

2) mass range (example is an Extrel quad)

$$f=880 \text{ kHz} \Rightarrow \Omega = (2\pi f) = 5.529 \times 10^6$$

$$V_{\max} = 3600 V_{0p}$$

$$r_0 = 4.14 \text{ mm}$$

$$\left(\frac{m}{z}\right)_{\max} = \frac{4eV_{\max}}{(0.706)r_0^2\Omega^2} = \frac{4(1.602 \times 10^{-19})(3600)}{(0.706)(0.00414)^2(5.529 \times 10^6)^2}$$

$$= 6.236 \times 10^{-24} \text{ kg/molecule} = 3755 \text{ Da}$$

49

Quad calcs:

2) mass range (example is an Extrel quad)

$$f=880 \text{ kHz} \Rightarrow \Omega = (2\pi f) = 5.529 \times 10^6$$

$$V_{\max} = 3600 V_{0p}$$

$$r_0 = 4.14 \text{ mm}$$

$$m/z \text{ max} = 3755 \text{ Da}$$

How much DC is needed?

$$U = a_u \frac{m r_0^2 \Omega^2}{z 8e} = (0.237) \left( \frac{3755}{1000} \frac{1}{6.023 \times 10^{23}} \right) \frac{(0.00414)^2 (5.529 \times 10^6)^2}{8(1.602 \times 10^{-19})}$$

$$U = 604 \text{ V}$$

50

Quad (mass filter) Resolution

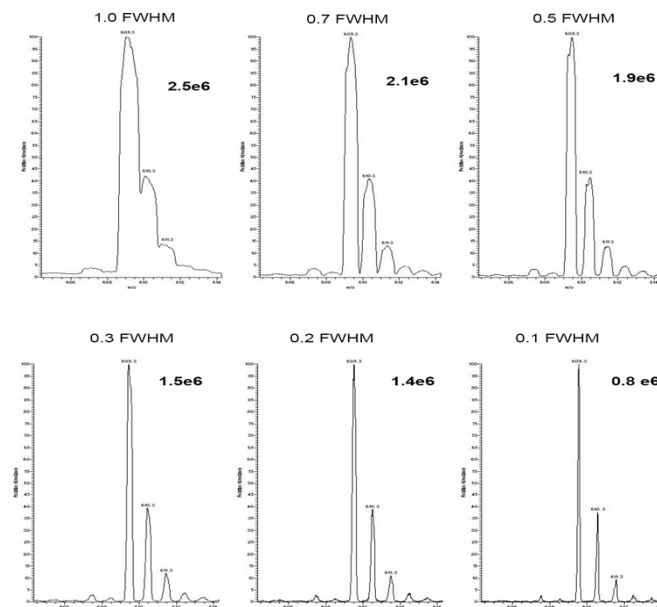
Resolution depends on (# cycles)<sup>2</sup>

Trade-off between transmission and resolution (acceptance angle)

Mechanical limits: non-ideal fields (round rods)  
rod alignment  
fringing fields

51

Mass Filter - Mass resolution, intensity and peakshape



### Quadrupoles

- 3 types: DC only, RF only,  
RF/DC (mass-selective stability)
- beam-type instrument
- Resolution controlled electronically (U/V scan)
- Resolution  $\propto (\# \text{ cycles})^2$
- m/z linear with U and V
- Focusing properties

53

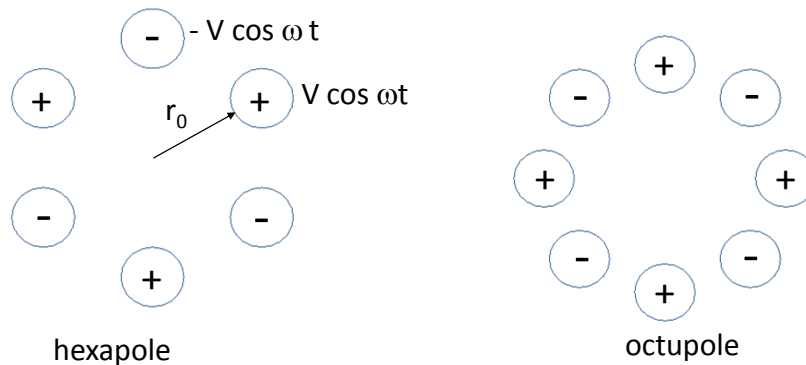
### Performance of Quadrupoles

- R=  $10^2$ - $10^4$
- 100 ppm accuracy
- m/z range <10,000
- LDR:  $10^7$
- Efficiency: <1-95%
- Speed: 1-20 Hz
- Ionizer: continuous
- Cost: low
- Size: benchtop

Very common mass analyzer

54

4. Higher order multipole ion guides (rf only)

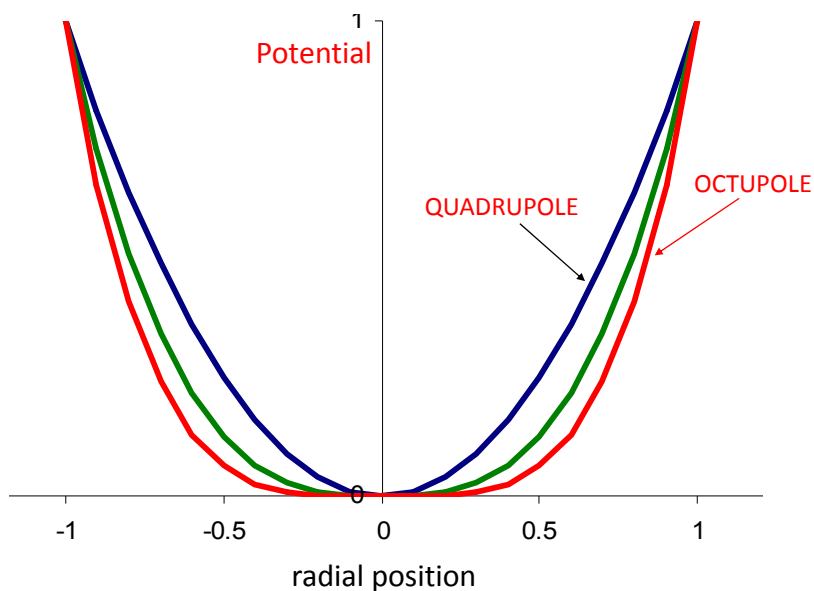


- collisional cooling (good for injection in TOF, sector, quad):  
 reduce velocity spread (thermal ions)
- more efficient collection of ions (compared to quad)

D. Gerlich, Adv. Chem. Phys. 82, 176 (1992).

55

collision energy more uniform in higher multipoles



56

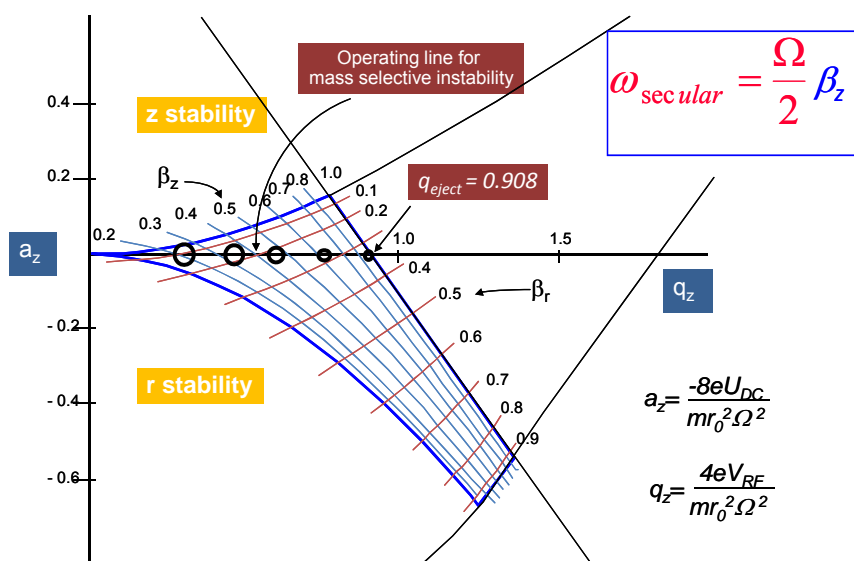
## 5. Quadrupolar Ion Trap

### History

1953 Wolfgang Paul	}	Mass-selective Detection
1963 Hans Dehmelt		
1968 Dawson & Whetten	}	Mass-selective Storage
1972 John Todd		
1972 Ray March		
<hr style="border-top: 1px dashed blue;"/>		
1984 George Stafford	}	Mass-selective Ejection

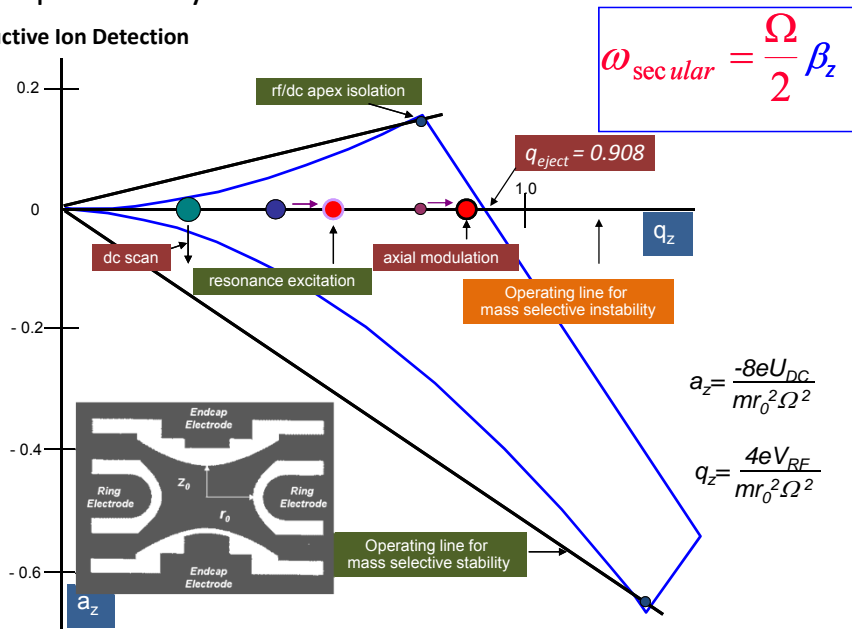
### Ion Trap

Stability diagram



### Ion Trap MS Analysis

#### Destructive Ion Detection



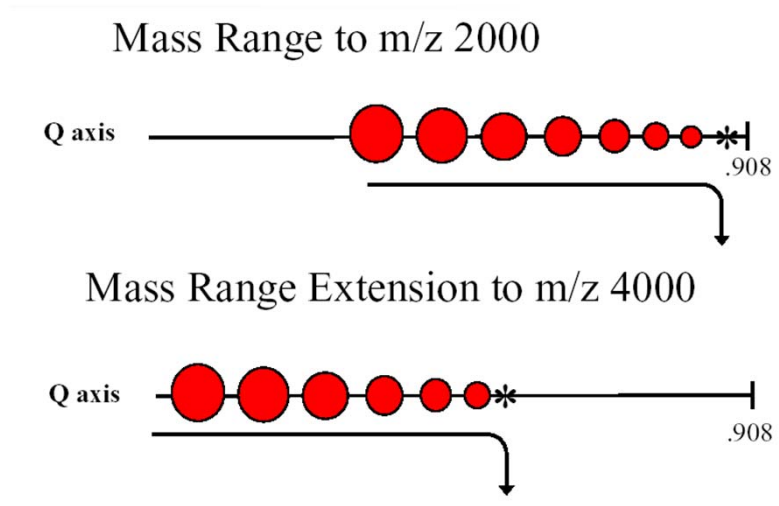
#### Ion Trapping

Ions can either be injected and created within the interior of the ion trap. They are confined by application of appropriate RF voltage and their position is maintained near the center of the ion trap.

PAUSE
STOP
RESTART

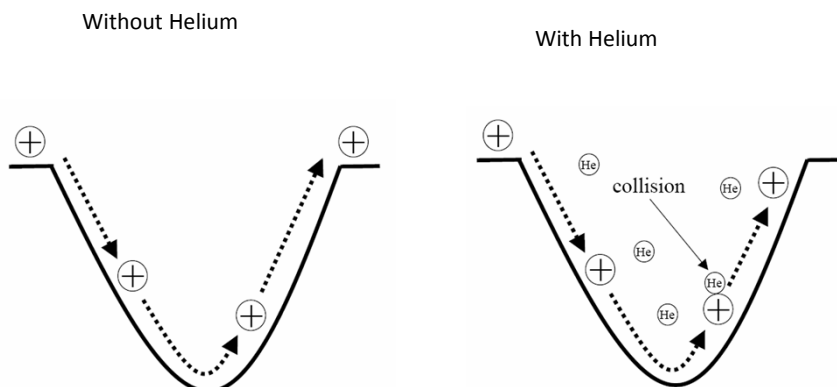
### Ion Trap Ejection Mode

Mass range extension using resonance ejection



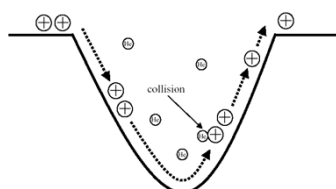
### Quadrupole Ion Trap – Collisions with Background Gas

Trapping injected ions

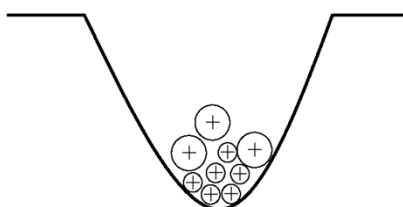
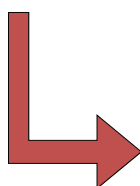
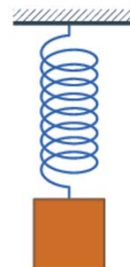


## Quadrupole Ion Trap

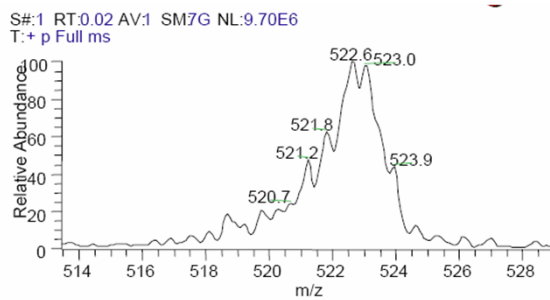
KE Damping



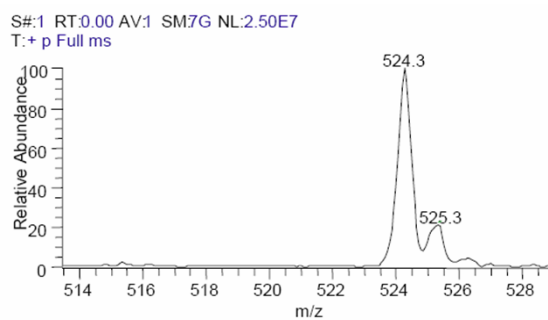
Collisions!!



Without He



With He

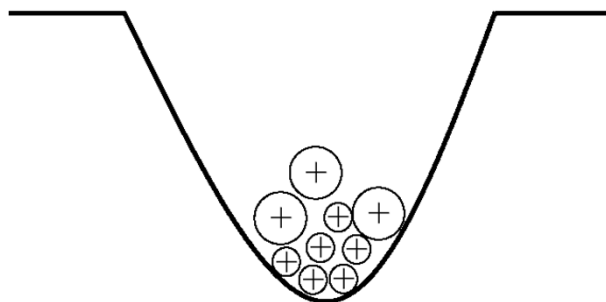




## Quadrupole Ion Trap

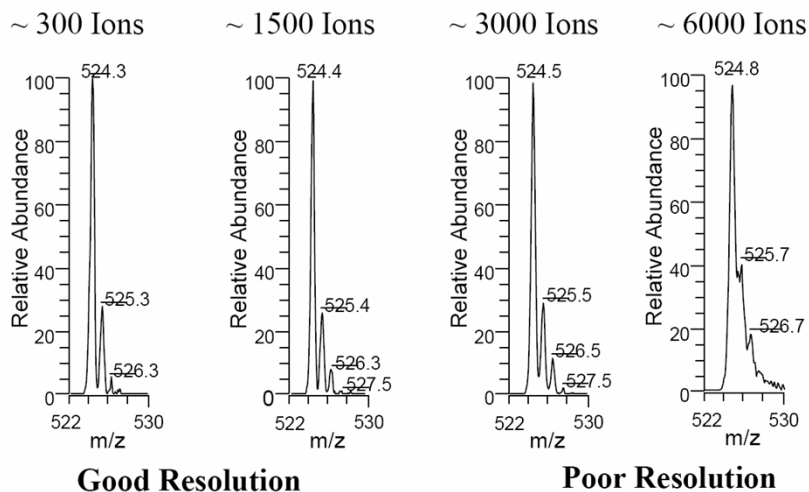
Trapping capacity vs. space charge

$$D_z = 2D_r = \frac{q_z V}{8}$$

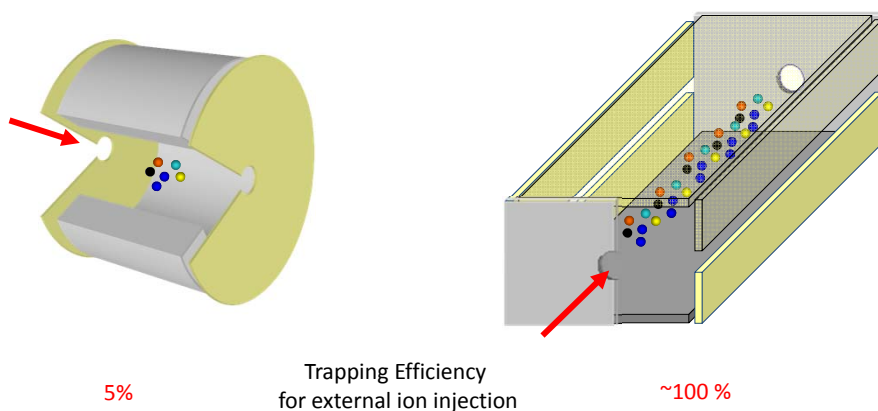


## Quadrupole Ion Trap

Trapping capacity vs. space charge – 3D Trap



## Why Linear Ion Trap?



## Theory of Quadrupole Ion Trap

Equations of motions

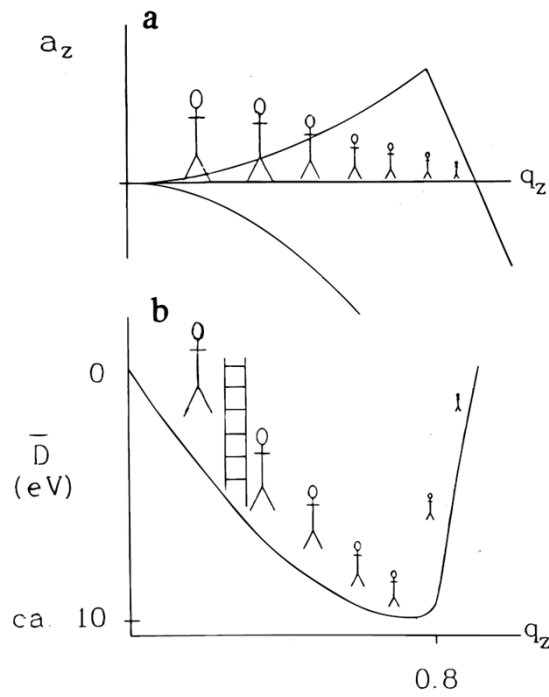
Acceleration of Ion expressed as a Second Order Differential Equation:

$$\frac{d^2z}{dt^2} = \frac{4e}{m(r_0^2 + 2z_0^2)} [U - V(t) \cos \Omega t] z \quad \text{Quadrupole Field}$$

$$+ \frac{e}{2mz_0} V_{aux}(t) \cos \Omega_{aux}(t) t \quad \text{Dipole Field}$$

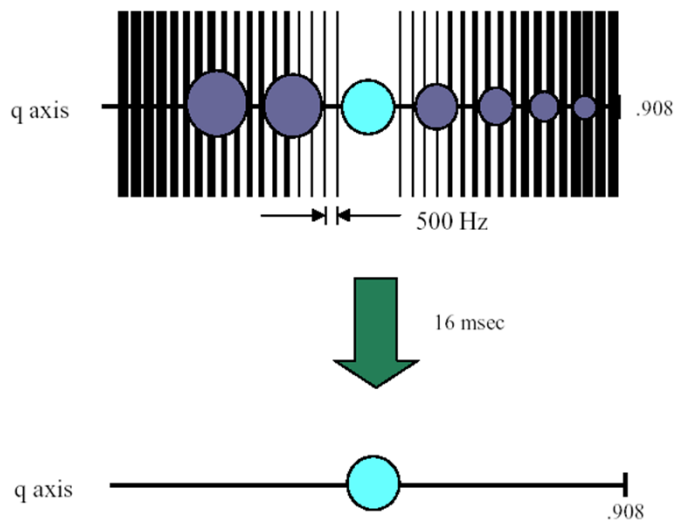
$$+ 1 - 1 \left( 1 - \sqrt{1 - \frac{4m_b}{m_i}} R(t) L(t) \right) \quad \text{Collision Term}$$

$$+ \frac{e}{4\pi\epsilon_0 m \sum_i \frac{1}{r - r_i^2}} \quad \text{Coulombic Term}$$



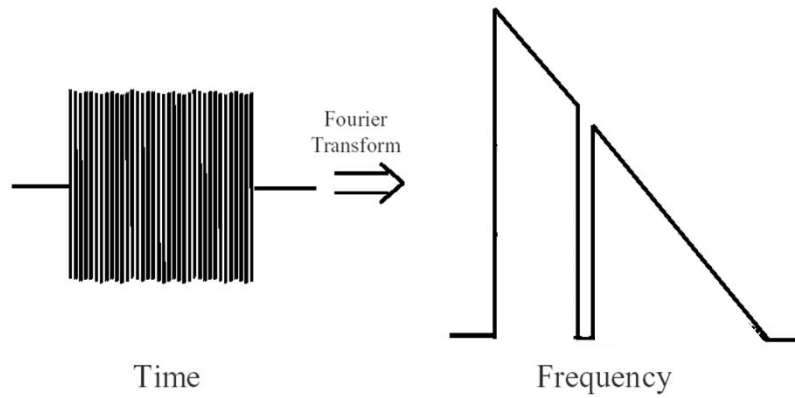
## Theory of Quadrupole Ion Trap

Isolation waveforms



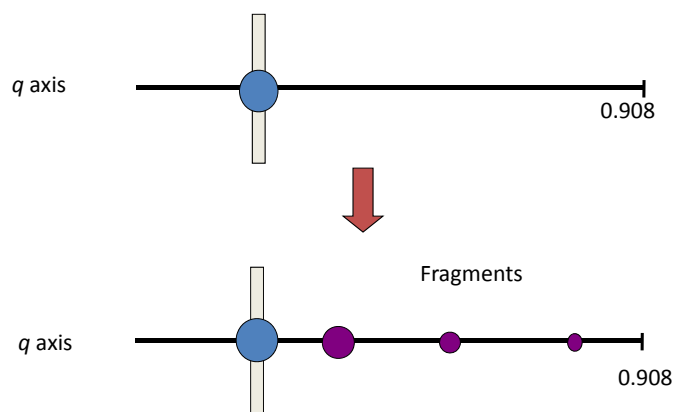
## Theory of Quadrupole Ion Trap

Isolation waveform



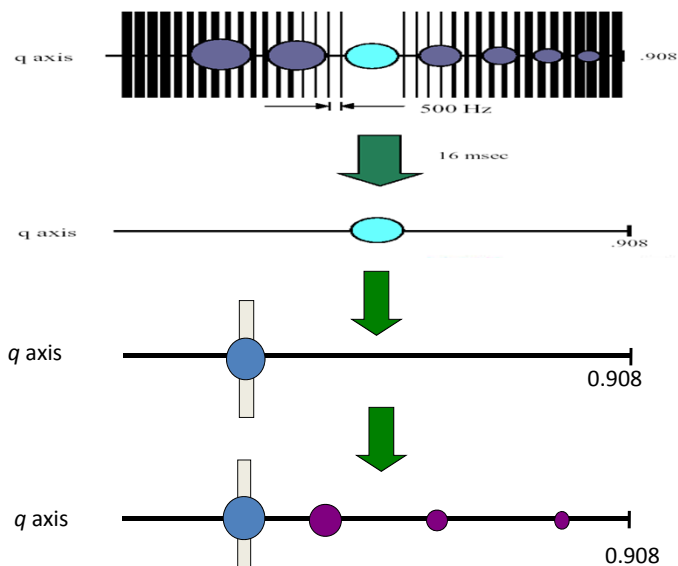
## Theory of Quadrupole Ion Trap

Resonance excitation



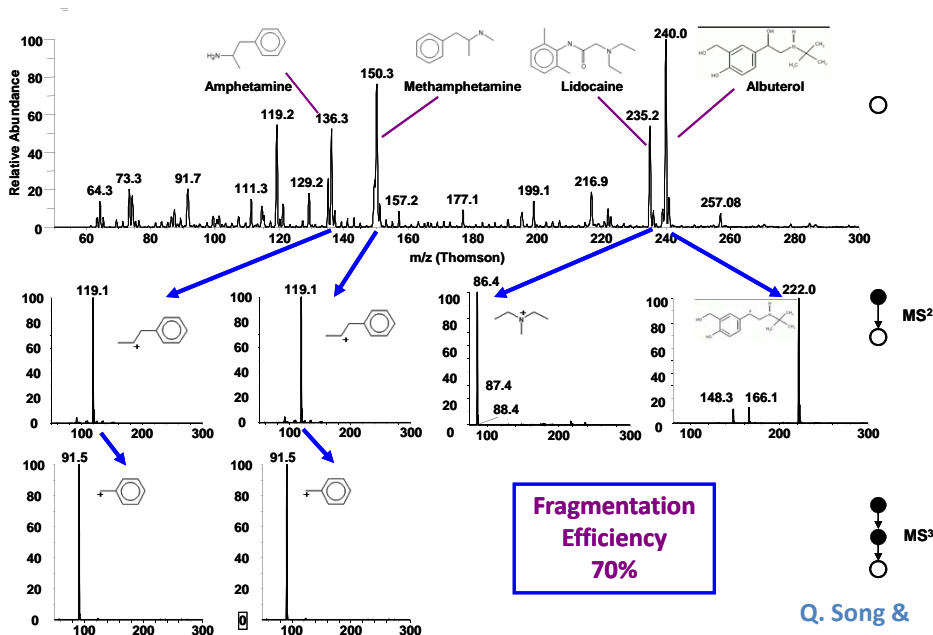
### Theory of Quadrupole Ion Trap

MS/MS



### ESI-RIT Instrument – MS<sup>n</sup> analysis to mixtures

ALMA mixture (100pg/ul)



### Performance of Quadrupole Ion Trap

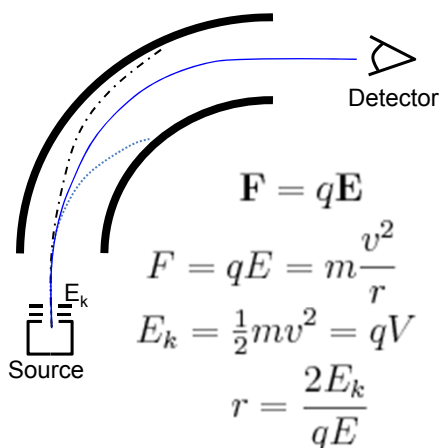
- R=  $10^3$ - $10^4$
- 50-100 ppm accuracy
- m/z range <100,000 (typ. 4000)
- LDR:  $10^2$ - $10^5$
  
- Efficiency: <1-95%
- Speed: 1-30 Hz
  
- Ionizer: pulsed and continuous
- Cost: low to moderate
- Size: benchtop

Very common mass analyzer

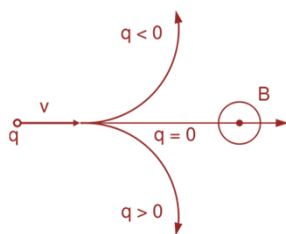
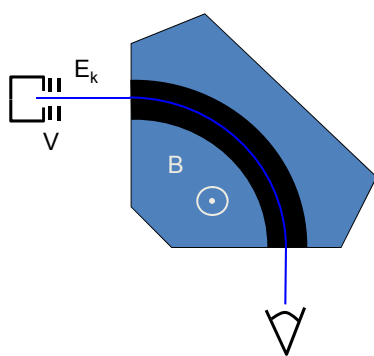
75

## Sectors

Separation in space  
 Electric Sector Mass Analyzer

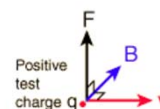
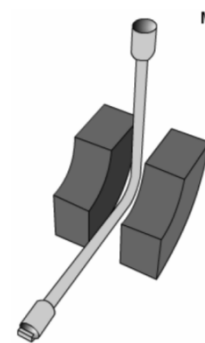


Separation in space  
 Magnetic Sector Mass Analyzer



Lorentz Force

$$\vec{F} = q\vec{v} \times \vec{B}$$



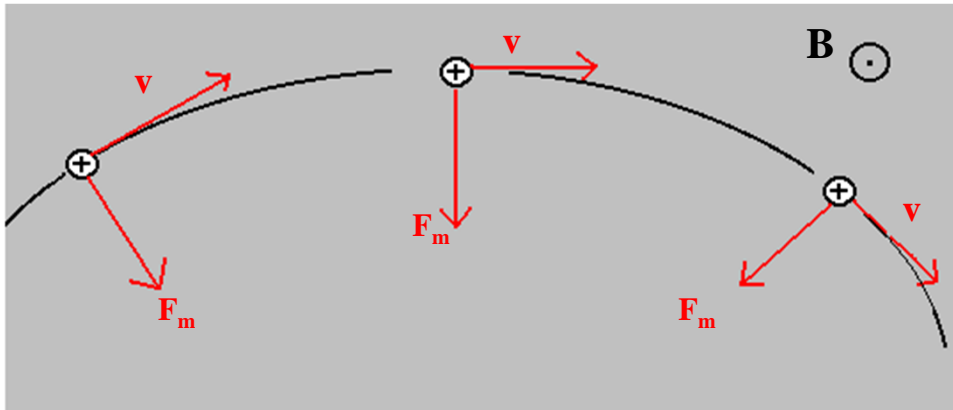
$$E_k = \frac{1}{2}mv^2 = eV_{\text{Detector}}$$

$$F = \frac{mv^2}{r} = Bev$$

$$\frac{m}{e} = \frac{B^2 r^2}{2V}$$

Magnetic Sector Mass Analyzer

+ ion moving through magnetic field with strength B



$F_m$  = magnetic force always acts perpendicular to direction of motion

\*Use right hand, Cross  $v$  into  $B$  with fingers Thumb points in dir. of  $F_m$

Uniform circular motion w/ radius  $r_m$  when:

$$F_m = Bzev = \frac{mv^2}{r_m}$$

Rearrange to get:  $\frac{mv}{z} = Br_m e$

So B sector is a momentum/charge analyzer, not a mass analyzer

Include KE from source:

$$KE = \frac{1}{2}mv^2 = zeV \Rightarrow v = \sqrt{\frac{2zeV}{m}}$$

$$\frac{m}{z} = \frac{B^2 r_m^2}{2V}$$



How do we get a  $m/z$  spectrum?

$$\frac{m}{z} = \frac{B^2 r_m^2}{2V}$$

Scan either:

B (vary mag. field: slow)  
V (vary acc. voltage: faster) AND / OR  
 $r_m$  (array detector)

*Performance of Sector magnets*

The sector magnet is lighter and hence more convenient, than the  $180^\circ$  magnet. It shares the property of bringing a divergent beam of ions to focus (to first order) — i.e. it is a direction focusing device. Ions entering normal to a magnetic field experience a force which depends upon the field strength, the magnitude of the charge and the velocity. Since the three vectors ( $B$ ,  $r$ ,  $v$ ) are mutually orthogonal, no change in velocity occurs and a circular path results.

Barber's rule states that for normal entry and egress, object, image and apex are collinear. The law is true for all sector angles and for both symmetrical and unsymmetrical arrangements of object and image.

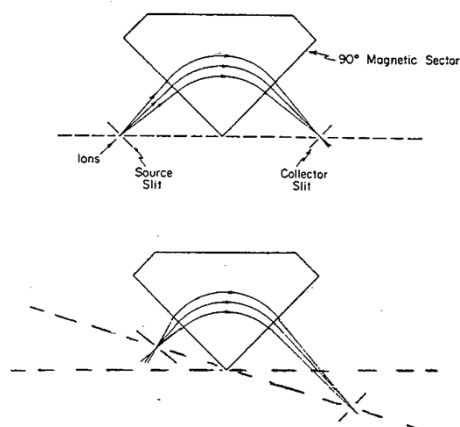


Fig. 4. Focusing action of a wedge-shaped (sector) magnetic field on a mono-energetic beam of ions, all of the same mass-to-charge ratio.

In fact, one desires both velocity and direction focusing. This is termed double focusing and is achieved with a suitable combination of a sector magnet and an electric sector. Each of these devices independently focuses for direction and together they give equal and opposite dispersions for velocity, i.e. they yield velocity focusing. Such double focusing instruments give high resolution. The fields may be arranged so that all masses are simultaneously subject to double focusing or, this may be true for just one mass/charge ratio at a time. They will be discussed later. However, it is important to recognize that there exist degrees of success in achieving both velocity and direction focusing. If focusing is to first order then the beam position is independent of the first power of velocity ( $v$ ) or direction ( $\alpha$ ), but dependent on the square terms. Focusing to second order means that a dependence exists on the third power of the parameters, etc.

There are two important geometries of double-focusing instruments from which all other designs have been developed, the *Nier-Johnson* geometry uses an electric sector (E) followed by a magnetic sector (B), the image of the electric sector being the object point of the magnetic sector, i.e. there is a point of intermediate focus. Along a plane normal to the ion beam and running through this focal point the beam is dispersed approximately linearly in terms of translational energy; the  $\beta$ -slit located at this point must be quite wide for high sensitivity. It is along this plane that the velocity dispersions due to the two sectors are equal and opposite for ions of the same  $m/z$  ratio. The final slit is located at the point at which a  $\Delta$  and  $\delta$  disappear to first order i.e. double-focussing is achieved.

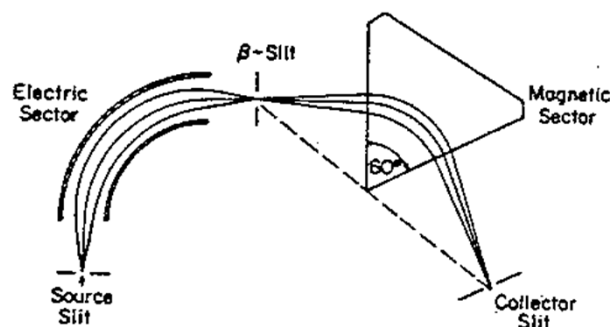


Fig. 8. Arrangement of the electric and magnetic fields for a double-focusing mass spectrometer of Nier—Johnson type geometry.

The *Mattauch-Herzog* geometry differs from the Nier-Johnson in many ways: (i) there is no point of intermediate focus, in fact the beam is approximately parallel between the sectors (ii) there is a plane of final focus, rather than a point and this allows imaging detectors to be used (note however, that the resolution is not the same at all points along the plane and is highest at the end which corresponds to maximizing the area of the sector covered by the ion beam).

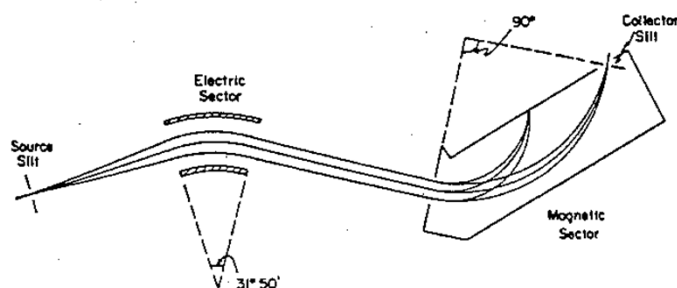
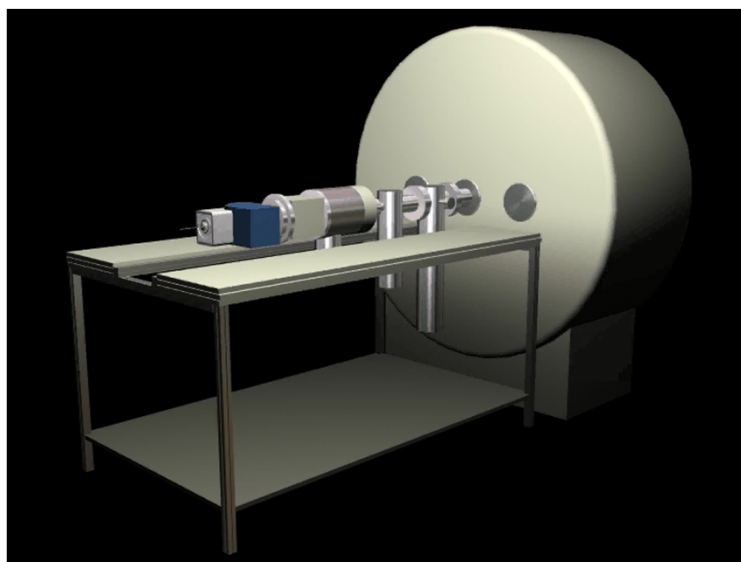


Fig. 9. Arrangement of the electric and magnetic fields for a double-focusing mass spectrometer of Mattauch—Herzog geometry.

#### 1. FT-ICR



Ion excitation for m/z analysis

Add power to excite ion packet to larger radii

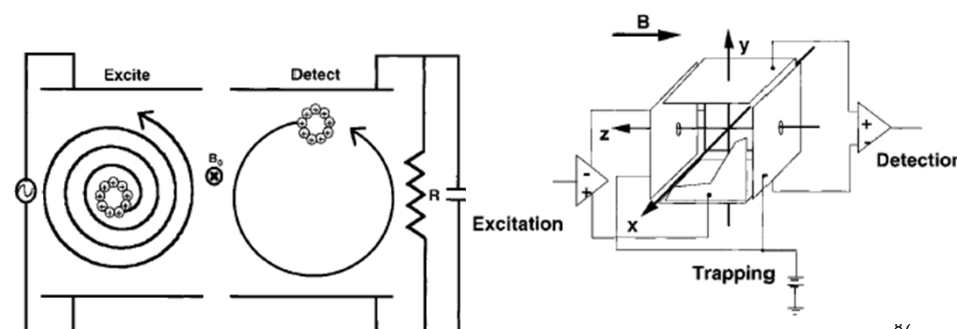
\*ions do not hit detector plates

(use dipolar excitation pulse)

$$r = \frac{V_{pp} T_{excite}}{2dB}$$

[m]                      [T]

Coherent ion packet oscillates at cyclotron freq



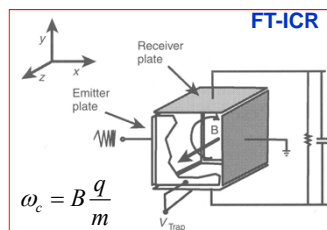
Mass Spectrom. Rev., 17, 1-35 (1998).

**2. The Orbitrap Mass Analyzer**

- Employs orbital trapping in an electrostatic field with potential distribution:

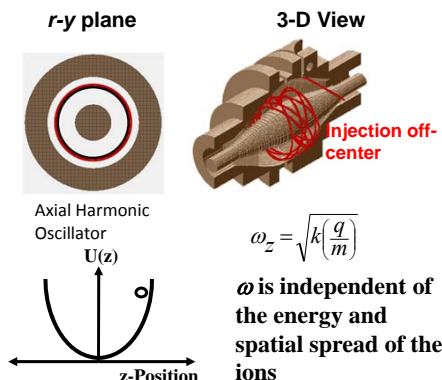
$$U(r,z) = \frac{k}{2} \left( z^2 - \frac{r^2}{2} \right) + \frac{k}{2} (R_m)^2 \ln \left[ \frac{r}{R_m} \right] + C$$

No cross terms in  $r$  and  $z$ . Thus the potential in the  $z$ -direction is exclusively quadratic and independent of  $r, \phi$  motion.



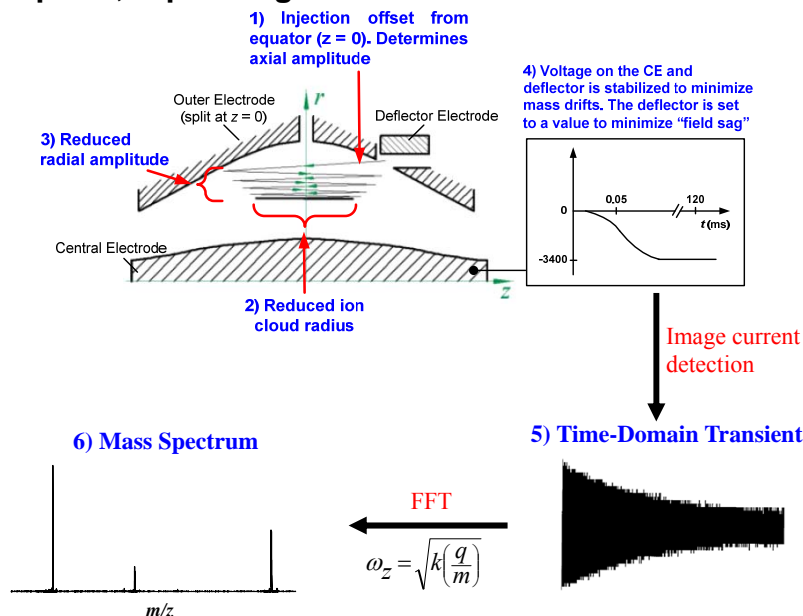
General features:

- High mass resolution (up to ~150,000)
- Increased space charge capacity at higher masses
- High mass accuracy (0.2-5ppm), dynamic range ( $10^3$ -  $10^4$ ) and upper mass limit ( $m/z$  6000)
- Small size and relatively low cost



1. Qizhi Hu, Robert J. Noll, Hongyan Li, Alexander Makarov, Mark Hardman and R. Graham Cooks, *J. Mass Spectrom.*, 2005, 40, 430; 2. Alexander Makarov, *Anal. Chem.*, 2000, 72, 1156. 3. Oksman, P., *Int. J. Mass Spectrom. Ion Processes*, 1995, 141, 67

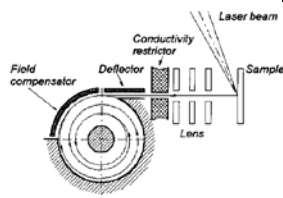
## Ion Capture, Squeezing and Detection



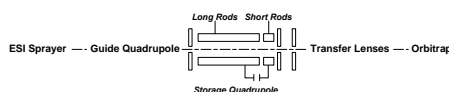
1. Qizhi Hu, Robert J. Noll, Hongyan Li, Alexander Makarov, Mark Hardman and R. Graham Cooks, *J. Mass Spectrom.*, 2005, 40, 430; 2. Alexander Makarov, *Anal. Chem.*, 2000, 72, 1156.

## Instrumentation

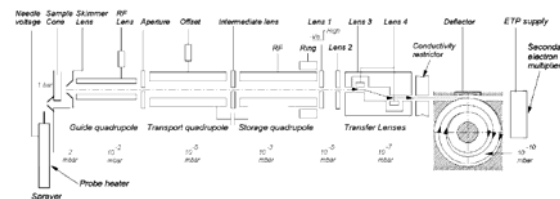
### Orbitrap Prototypes



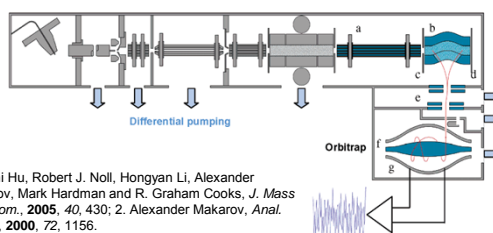
(a) First API-Orbitrap Prototype Instrument



(b) Second API-Orbitrap Prototype Instrument



### Commercial LTQ-Orbitrap



1. Qizhi Hu, Robert J. Noll, Hongyan Li, Alexander Makarov, Mark Hardman and R. Graham Cooks, *J. Mass Spectrom.*, 2005, 40, 430; 2. Alexander Makarov, *Anal. Chem.*, 2000, 72, 1156.

#### Disadvantages of FT-ICR:

- Small space charge capacity
- High complexity and cost.

#### Disadvantages of the Paul Trap:

- Unit resolution
- Insufficient mass accuracy (10 ppm at best)
- Small space charge capacity.

• The Orbitrap is a complementary alternative to these methods

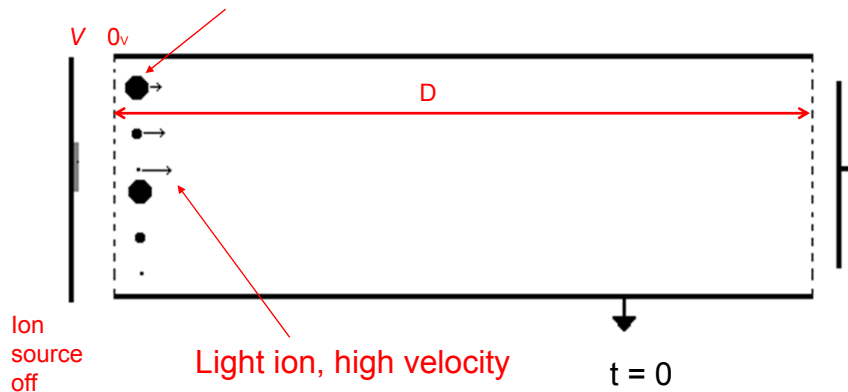
• It employs **dynamic ion trapping** in an electrostatic field.

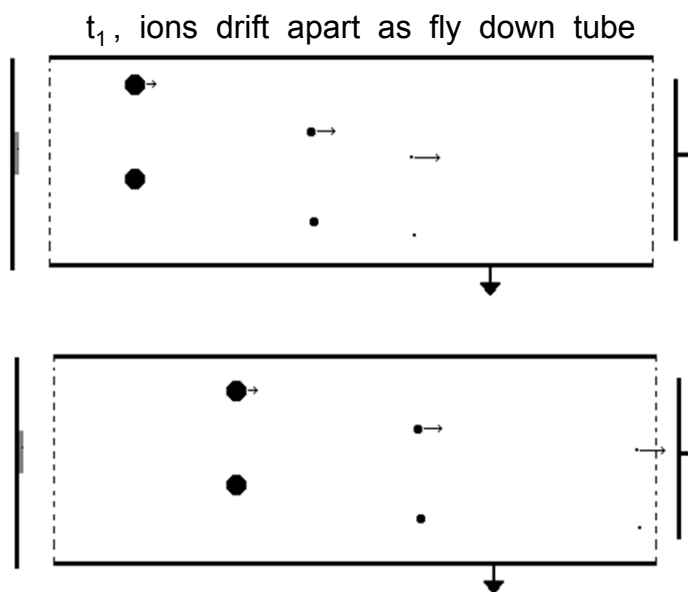
# TOF

$$KE = qV = \frac{1}{2}mv^2 \quad v = \sqrt{\frac{2qV}{m}}$$

$$t = \frac{D}{v} = \frac{D\sqrt{m}}{\sqrt{2zeV}} \quad \frac{m}{z} = \frac{2eVt^2}{D^2}$$

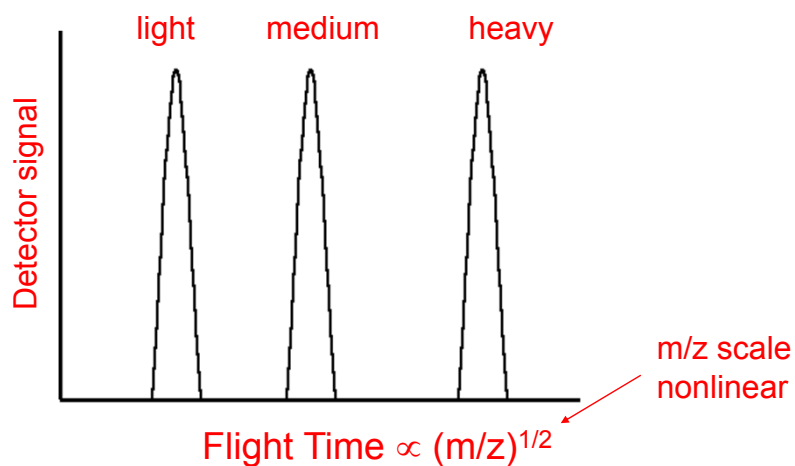
Heavy ion, low velocity





$t_2$ , light ions near detector, heavy ions still in tube

93



Detect "all" ions that entered flight tube

Full  $m/z$  range but *no scanning*

94

### Evolution of TOF from 1950 to 2000

- ⌞ **1946** Stephens presented concept of linear TOF MS
- ⌞ **1953** Woff and Stephens published design and spectra from linear TOFMS
- ⌞ **1955** First commercial linear TOF based on Wiley and McLaren 's design
- ⌞ **1973** Reflectron-TOF by Mamyrin
- ⌞ **1986** TOF/TOF by Brucat
- ⌞ **1988** MALDI source by Karas, Hillenkamp, then MALDI-TOF
- ⌞ **1989** Dawson and Guilhaus described EI+orthogonal TOF  
ESI+orthogonal TOF by Dodonove
- ⌞ **90's** QqTOF

### Factors Contributing to TOF-MS Renaissance

- High mass**
  - The need to measure the mass of biological molecules
  - Discover MALDI ionization by Karas and Hillenkamp
  - Quadrupoles and sectors have fundamental high mass limit
- Digital electronics**
  - Advances in the speed and data handling of computers
  - Progress in high speed timing electronics
  - nanosecond digitizers, focal plane detector, affordable laser
- Speed**
  - Detect ions quasi-simultaneous
  - Well in the time-frame of chromatography

Gilhaus et al. *Rapid Commun. Mass Spectrom.* **1997**,11, 951-962



Reduced Eqn for TOF

$$\frac{m}{z} = 1.92 \frac{V t^2}{L^2}$$

Volts     $\mu\text{s}$   
cm

- m/z scale non-linear
- time scale shrinks at higher m/z

To observe very high m/z, just wait longer

No (theoretical) limit to mass range

- detector response poor
- peaks very close in time

97

<u>m/z</u>	<u>t (<math>\mu\text{s}</math>)</u>	<u><math>\Delta t</math> (ns)</u> ~ time resolution needed	
$^{14}\text{N}^+$	5.20	180	
$^{15}\text{N}^+$	5.38		
$^{207}\text{Pb}^+$	20.00	50	
$^{208}\text{Pb}^+$	20.05		
500	31.09	30	
501	31.12		
20,000	196.623	5	Create ion pulse < 5 ns Time constants of electronics need to be faster than 5 ns
20,001	196.628		

98

Effect of Instrument Parameters on Resolution

$$m/z = m = \frac{2 V t^2}{L^2} = 2 V t^2 L^{-2}$$

$$dm = \frac{2 t^2}{L^2} dV + \frac{2 V}{L^2} (2t) dt + 2 V t^2 (-2L^{-3}) dL$$

$$\frac{dm}{m} = \frac{dV}{V} + \frac{2dt}{t} + \frac{2dL}{L}$$

Small dL  
All ions same tube length  
Long tube

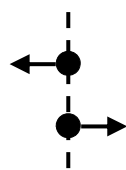
Small KE spread  
Large KE, high V  
(2 – 10 kV)

Fast time response  
Long flight time, long tube

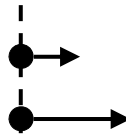
99

What causes poor resolution (time spread)?

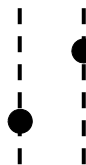
•Direction spread



•Velocity spread

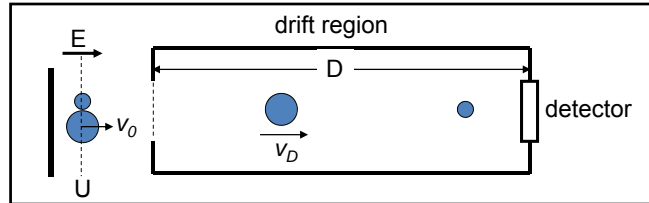


•Position spread



100

TOF Mass Spectrometer– Theory of Work



$$TOF = t_{delay} + t_{accel} + t_D + t_{detect}$$

$$qU = \frac{1}{2}mv_D^2 \quad t_D = \frac{D}{\sqrt{2U}} \left( \frac{m}{q} \right)^{1/2}$$

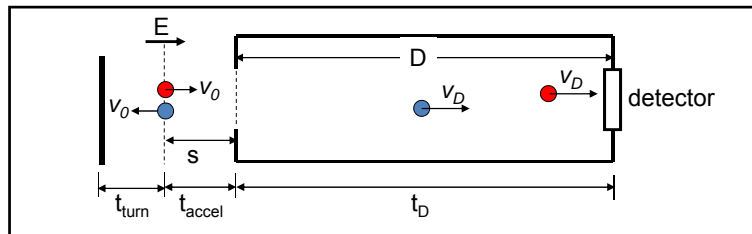
$t_{delay}$  any delays between ionization and acceleration

$t_{accel}$  time to reach full velocity before enter drift region  $t_{accel} = \frac{v_D - v_0}{E} \left( \frac{m}{q} \right)$

$t_D$  drift time in the 100  $\mu$ s time frame  $t_D = \frac{D}{\sqrt{2U}} \left( \frac{m}{q} \right)^{1/2}$

$t_{detect}$  detector response time (1-5 ns)

Direction Spread: the Turn-Around Problem



If  $U_0 =$  initial kinetic energy, then  $t_{turn} = \frac{2\sqrt{2mU_0}}{Eq}$

➤  $t_{turn}$  can be decreased by increasing E or decrease  $U_0$

$$t_D = \sqrt{\frac{2m(EqS + U_0)}{Eq}}$$

➤ Relative contribution of  $t_{turn}$  can be decreased by increasing D

$$t = \frac{(2m)^{1/2} \left[ \left( U_0 + qES \right)^{1/2} \pm U_0^{1/2} \right]}{qE} + \frac{(2m)^{1/2} D}{2(U_0 + qES)^{1/2}}$$

### Resolving Power of TOF

$$m \propto t^2 \Rightarrow \frac{dm}{m} = \frac{2dt}{t} \quad \text{or} \quad \frac{m}{\Delta m} = \frac{t}{2\Delta t}$$

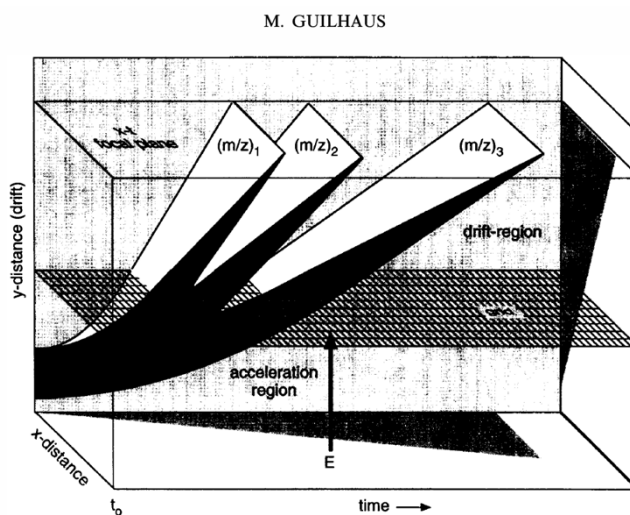
$\Delta t$ : the full-width at the maximum height of the peak (FWHM)

$$TOF = t_{delay} + t_{accel} + t_D + t_{detect}$$

Contributions to  $\Delta t$ :

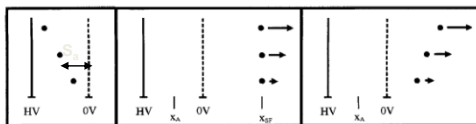
1. timing/duration of gating and detection interval
2. position spread
3. direction spread (turn around time)
4. initial velocity spread

$$t = \frac{(2m)^{1/2} \left[ (U_0 + qES)^{1/2} \pm U_0^{1/2} \right]}{qE} + \frac{(2m)^{1/2} D}{2(U_0 + qES)^{1/2}}$$



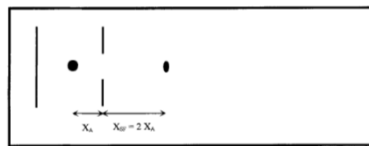
Mass-dispersed space-time trajectories

Initial Position Spread and Spatial Focusing

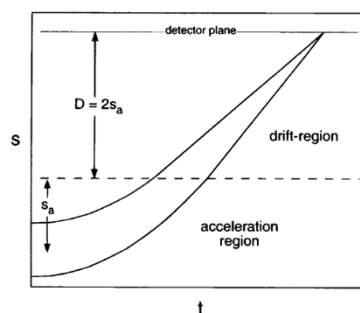


$$\frac{dt}{ds_a}(U_0 = 0) = \sqrt{\frac{m}{2qEs_a}} \times \left(1 - \frac{D}{2s_a}\right)$$

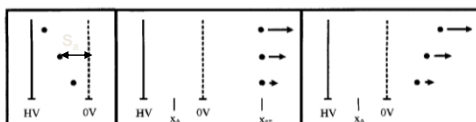
$$\frac{dt}{ds_a} = 0 \Rightarrow D = 2S_a$$



One stage acceleration  
 Spatial focus at  $D=2S_a$

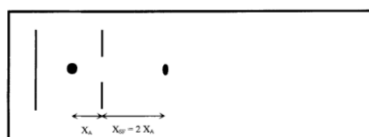


Initial Position Spread and Spatial Focusing

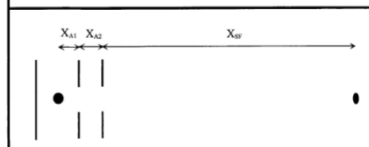


$$\frac{dt}{ds_a}(U) = \sqrt{\frac{m}{2qEs_a}} \times \left(1 - \frac{D}{2s_a}\right)$$

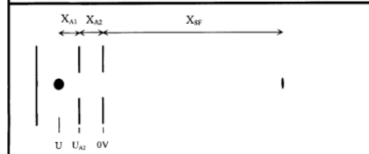
$$\frac{dt}{ds_a} = 0 \Rightarrow D = 2S_a$$



One stage acceleration  
 Spatial focus at  $D=2S_a$



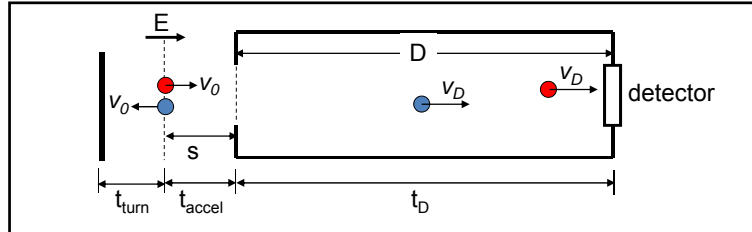
double stage acceleration



Double stage acceleration with  
 second order space focus

Bosel et al. *Int. J. Mass Spectrom. Ion Processes* **1992**, 112, 121

Direction Spread: the Turn-Around Problem



If  $U_0$  = initial kinetic energy, then  $t_{turn} = \frac{2\sqrt{2mU_0}}{Eq}$

➤  $t_{turn}$  can be decreased by increasing E or decrease  $U_0$

$$t_D = \sqrt{\frac{2m(EqS + U_0)}{Eq}}$$

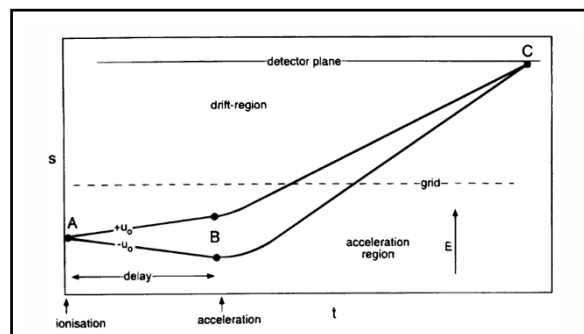
➤ Relative contribution of  $t_{turn}$  can be decreased by increasing D

$$t = \frac{(2m)^{1/2} \left[ (U_0 + qES)^{1/2} \pm U_0^{1/2} \right]}{qE} + \frac{(2m)^{1/2} D}{2(U_0 + qES)^{1/2}}$$

Initial Velocity Distribution and Time-lag Focusing

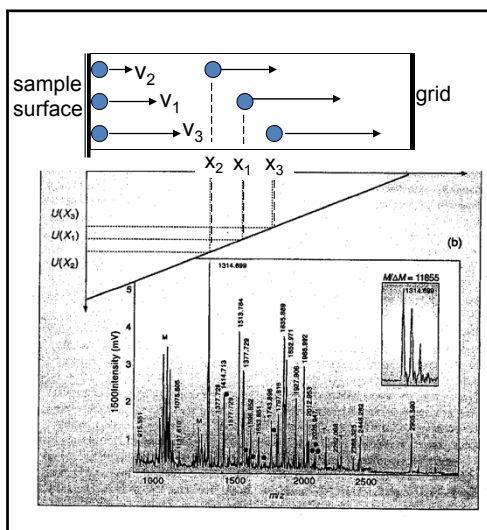
Time-lag focusing: delay between ion ionization and extraction (Wiley & McLaren)

Convert velocity distribution to spatial distribution, then use spatial focusing



- Focus is m/z dependent
- enhanced resolving power for a limited mass range
- Does not solve turn-around problem

Initial Velocity Distribution & Delayed Extraction for MALDI/TOF



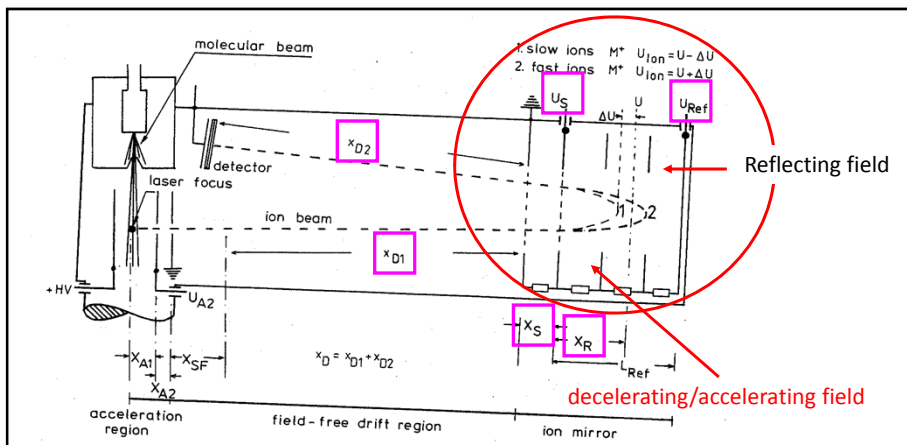
Correlated space and energy distributions  
 > Ions with larger initial velocity acquires less energy from the field

Difference between time-lag focusing  
 > In time-lag focusing: no correlation between energy and space

- Focus is still m/z dependent
- No turn-around problem for MALDI

Colby et al. *Rapid Commun. Mass Spectrom.* **1994**, 8, 865-868

Energy Correction by Reflectron (Mamyrin et al.)



- ✓ Reflectron consists two fields (three electrodes)
- ✓ By properly choose parameters (in box), energy distribution (5%) can be corrected
- ✓ Increase fly length without increase size, resolution can reach 20,000
- ✓ Can not solve turn-around problem (works well with ions generate from surface)

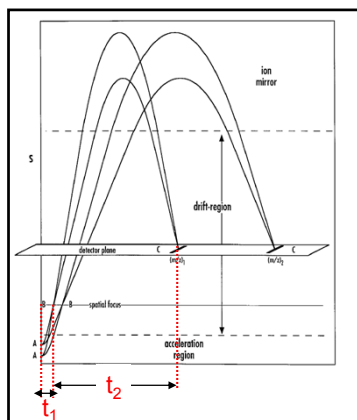
Bosel et al. *Int. J. Mass Spectrom. Ion Processes* **1992**, 112, 121

### Reflectron Continued...

for energy compensation ion mirror:  
 second-order focus ion source

$$t = \left( \frac{m_1}{2eV} \right)^{1/2} [L_1 + L_2 + 4d]$$

$L_1$ : drift region before reflection  
 $L_2$ : drift region after reflection  
 $d$ : penetration depth in the reflectron  
 $V$ : acceleration voltage  
 Optimal focusing when  $L_1 + L_2 = 4d$



Resolution for a reflectron:

$$\frac{\Delta t}{t} = \underbrace{\frac{1}{4} \left( \frac{\Delta U}{U} \right)^2 \frac{t_1}{t}}_{\text{"second-order term of ion source"}} + \underbrace{\frac{3}{16} \left( \frac{\Delta U}{U} \right)^3 \frac{t_2}{t}}_{\text{"third-order term of ref"}} + \underbrace{\frac{x_{A1}}{U_{A1}} (MU_i)^{1/2} \frac{1}{t}}_{\text{"turn around time"}} + \underbrace{\frac{\Delta t_{fix}}{t}}_{\text{"laser pulse width"}}$$

Bosel et al. *Int. J. Mass Spectrom. Ion Processes* **1992**, 112, 121

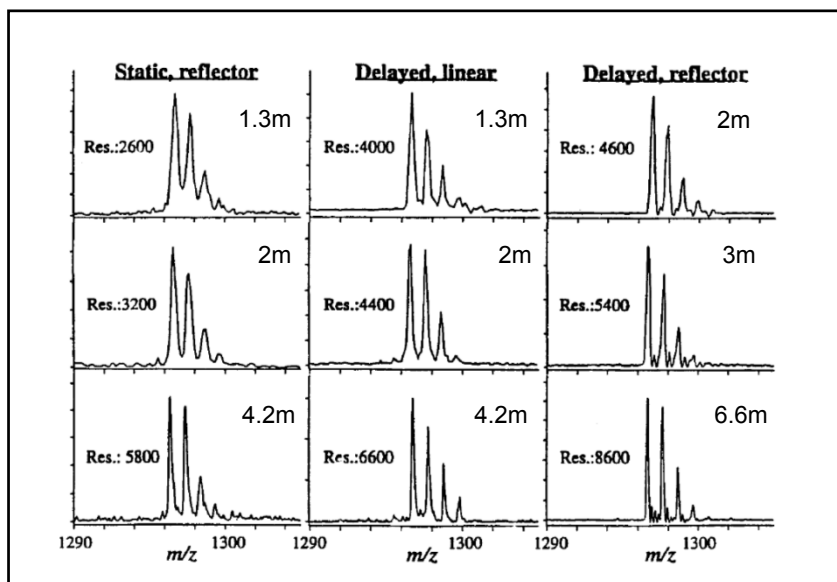
Table 1 Limiting factors for mass resolution of reflectron TOF with a laser ionization source. The values of  $\Delta t$  are determined for ions with  $M=106$ , an ion energy of 700eV and a flight time of 60  $\mu s$ .

Limitations for mass resolution ( $R < 3000$ )		
$\Delta t$ (laser pulse width)	5-8 ns	commercial dye laser
$\Delta t$ (detector rise time)	1.4 ns	
$\Delta t$ (turn around time)	5 ns	$T=300$ K
$\Delta t$ (Re-TOF third-order term)	< 1 ns	
$\Delta t$ (Re-TOF geometry)	5 ns	Reflector with grids
$\Delta t$ (space charge)	12 ns	$10^4$ ions, focus $r=0.05$ mm, $l=1$ mm
Optimization for high mass resolution ( $R > 10\,000$ )		
$\Delta t$ (laser pulse width)	1.5 ns	Pulse cutting
$\Delta t$ (turn around time)	< 1 ns	Supersonic jet cooling
$\Delta t$ (space charge)	< 1 ns	Optimized focus size
$\Delta t$ (Re-TOF grid)	0 ns	Gridless reflector
Result: for $M=106$ ( <i>p</i> -xylene): $\Delta t_{FWHM}=3.2$ ns, $\Delta t_{unit}=310$ ns		
$R_{50\%} = M \Delta t_{unit} / \Delta t_{FWHM} = 10270$		

Bosel et al. *Int. J. Mass Spectrom. Ion Processes* **1992**, 112, 121

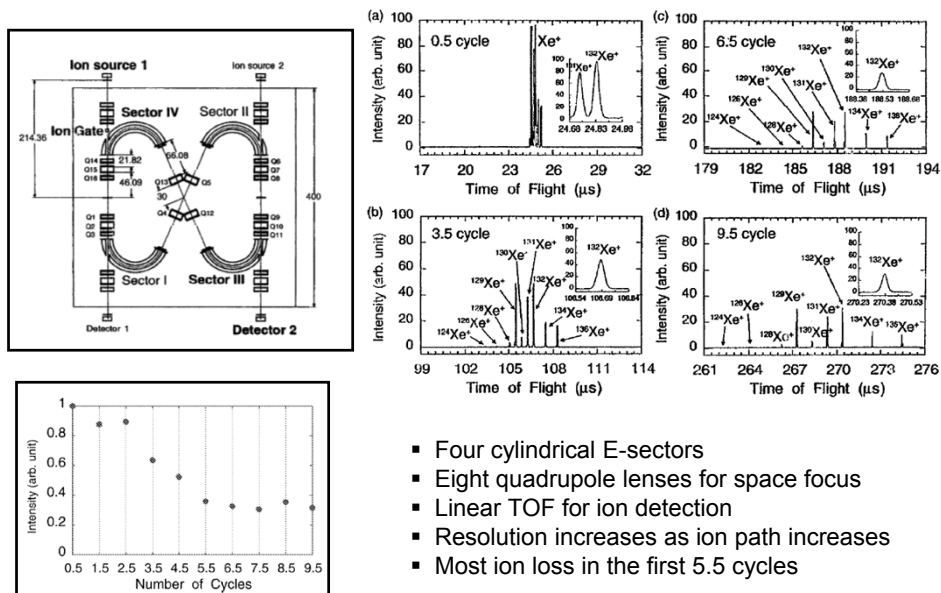


Comparison of the Resolution and S/N for Angiotensin I



Vestal et al. *Rapid Commun. Mass Spectrom.* **1995**, 9, 1044

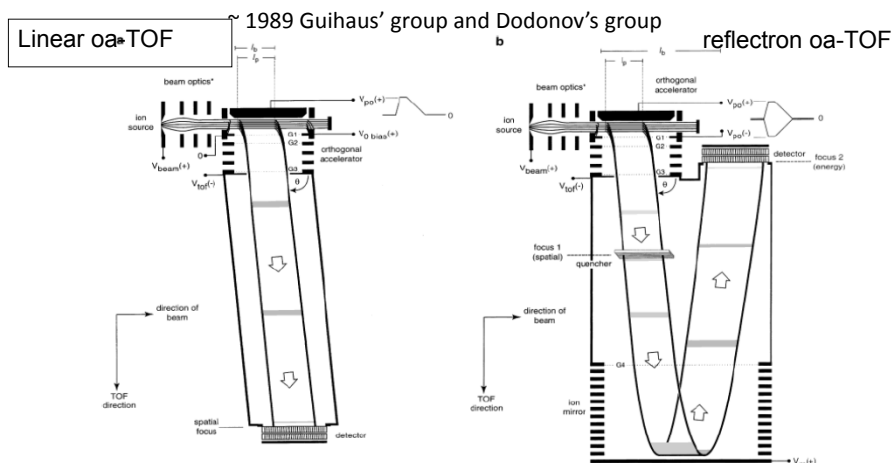
Multiturn TOF for High Resolution



- Four cylindrical E-sectors
- Eight quadrupole lenses for space focus
- Linear TOF for ion detection
- Resolution increases as ion path increases
- Most ion loss in the first 5.5 cycles

Toyoda et al. *J. Mass Spectrom.* **2000**, 35, 163

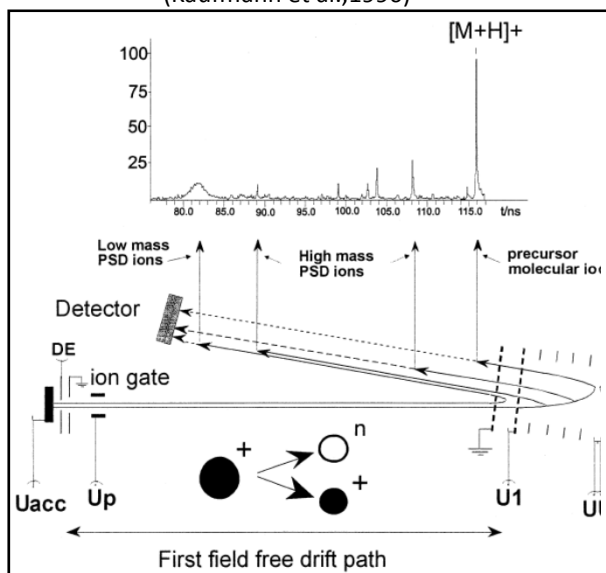
**Orthogonal Acceleration TOF- Solutions for Continuous Ionization**



Guihaus et al., *Mass Spectrom. Rev.*, **2000**, 19, 65-107

**MS<sup>n</sup> Capabilities of TOF – Post Source Decay**

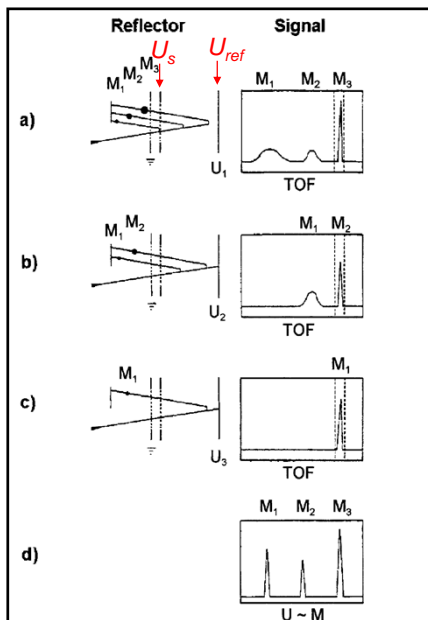
(Kaufmann et al., 1996)



- PSD: parent ions acquired sufficient internal energy during the desorption process, fragmented in first field free region.
- Fragment ions have the same velocity as their precursor ions but have different kinetic energy as function of their mass. (can not use linear TOF)
- Lighter ions reach earlier than heavier ions in ref-TOF
- For linear field reflectron, best focus when  $L=4d$ .
- Bad resolution with one reflectron voltage.

Chaurand et al. *J. Am. Soc. Mass Spectrom.* **1999**, 10, 91

### Scan Method for Secondary Mass Spectra



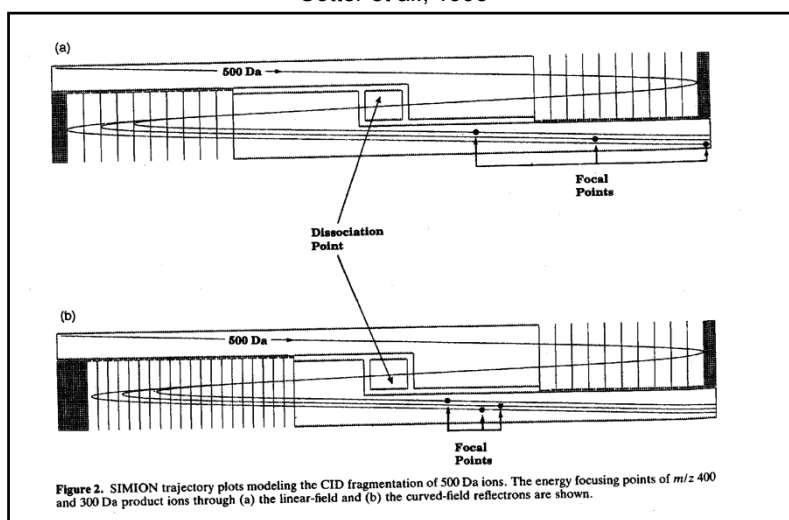
Weinkauf et al., 1989

- Scan  $U_{ref}$  and keep  $U_{ref}/U_s$  constant as parent ion.
- Fragment ions penetrate same distance in reflectron, thus have same resolution as parent ion.
- Lose major advantage of TOF: detect all masses quasi-simultaneously

Bosel et al. *Int. J. Mass Spectrom. Ion Processes* **1992**, 112, 121

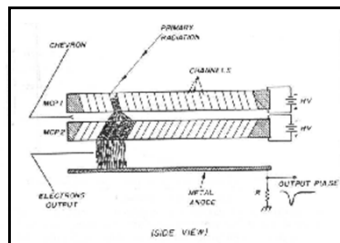
### Curved-Field Reflectron for Secondary Mass Spectra

Cotter et al., 1993



Cotter et al. *Rapid Commun. Mass Spectrom.* **1993**, 7, 1037-1040

### Detection in TOF



- multi-channel plate in "Chevron" arrangement
- 10-25  $\mu\text{m}$  channels inclined @ 8-12°
- Single ion impact  $\rightarrow$  1-5 ns pulse width
- detect single ion impact (problem at high m/z)
- Flat conversion surface
- Large area, detect large ion packets
- Better use smallest channel diameter (time spread)

### Digitizers in TOF

#### Time-to-digital converter (TDC)

- for low ion currents (ESI)
- Register events of pulses
- Good S/N
- Good time resolution (<0.3 ns)
- Limited dynamic range due to dead time
- Can only register one ion at a time

#### Integrating Transient Recorder (ITR)

- For high ion currents (MALDI, ICP)
- Analog systems digitize ion current from MCP.
- Expensive
- Inherent background noise
- Low repeat rates

### Feature of Merit -- TOF vs. QIT

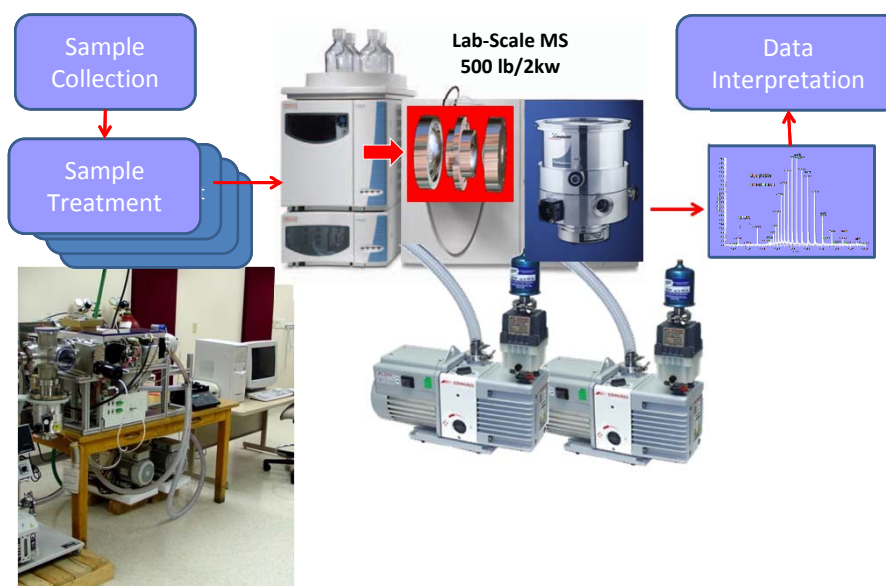
	TOF	Ion-trap
Mass resolving power	10 <sup>3</sup> -10 <sup>4</sup>	10 <sup>3</sup> -10 <sup>4</sup>
Mass accuracy	5-50 ppm	50-100 ppm
Mass range	>10 <sup>5</sup>	1.5 x 10 <sup>5</sup>
Linear dynamic range	10 <sup>2</sup> -10 <sup>6</sup>	10 <sup>2</sup> -10 <sup>5</sup>
precision	0.1-1%	0.2 -5%
Abundance sensitivity	Up to 10 <sup>6</sup>	10 <sup>3</sup>
Efficiency (transmission x duty cycle)	1-100%	<1- 95%
speed	10-10 <sup>4</sup> Hz	1-30 Hz
Compatibility with ionizer	Pulsed and continuous	Pulsed and continuous
cost	Moderate-high	Low to moderate
Size/weight/utility requirements	benchtop	benchtop

McLucky et al. *Chem. Rev.* **2001**, 101, 571-606

### Suggested Reading

- Weickhardt et al., *Mass Spectrom. Rev.*, **1996**, 15, 139-162, "Time-of-flight mass spectrometry: state-of-art in chemical analysis and molecular science"
- Bosel et al., *Int. J. Mass Spectrom. Ion Processes*, **1992**, 112, 121-166, "Reflectron time-of-flight mass spectrometry and laser excitation for analysis of neutrals, ionized molecules and secondary fragments"
- Guihaus et al., *Mass Spectrom. Rev.*, **2000**, 19, 65-107, "Orthogonal acceleration time-of-flight mass spectrometry"
- Chernushevich et al., *J. Mass Spectrom.*, **2001**, 36, 849-865, "An introduction to quadrupole-time-of-flight mass spectrometry"
- McLuckey et al., *Chem. Rev.*, **2001**, 101, 571-606 "Mass Analysis at the Advent of the 21<sup>st</sup> Century"

### MS Instrumentation and Miniaturization



### Tiny TOF

Cotter, Johns Hopkins  
 Higher Order KE Focusing  
 5 cm Endcap Reflection

$m/z$  70,000,  $R = 70$

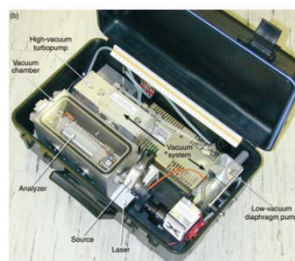
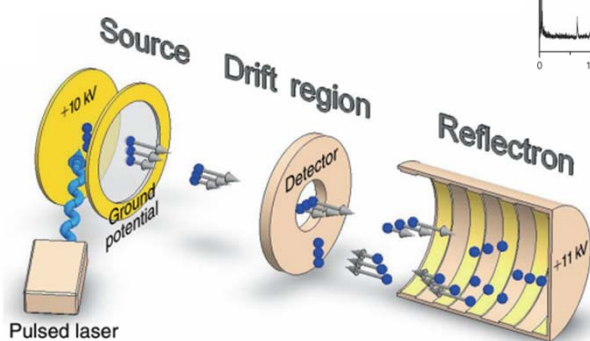
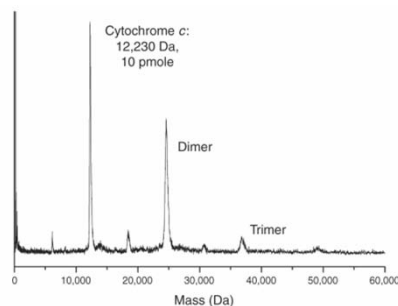


Figure 3

### Double Focusing

Sinha, JPL  
 Mattauch-Herzog  
 Light B Sector

$m/z$  300,  $R = 300$

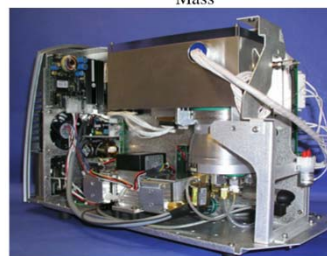
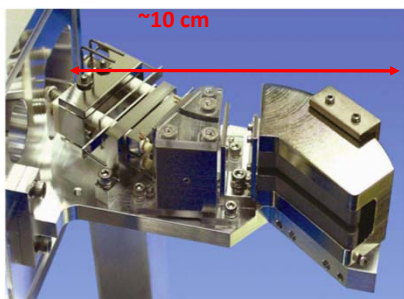
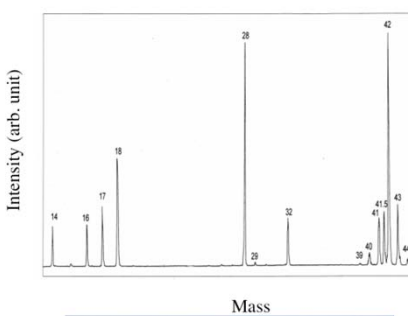
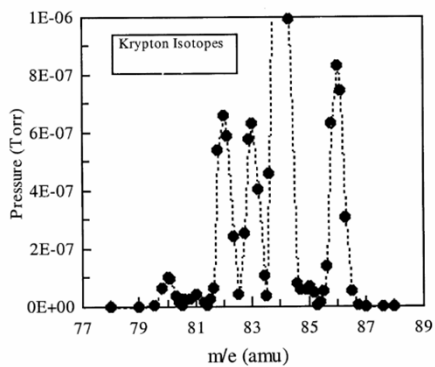
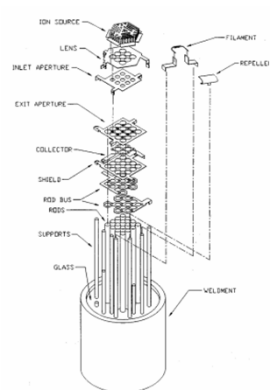


Figure 3

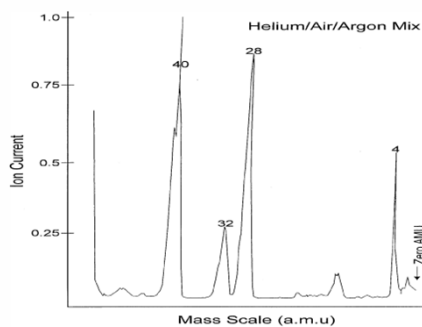
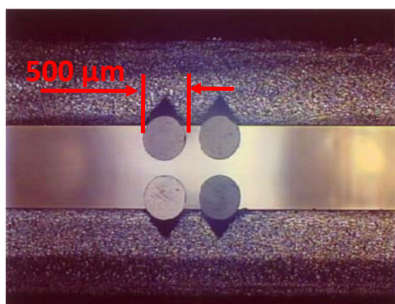
## Quadrupole Filter Array

Ferran  
0.5 ID Rod

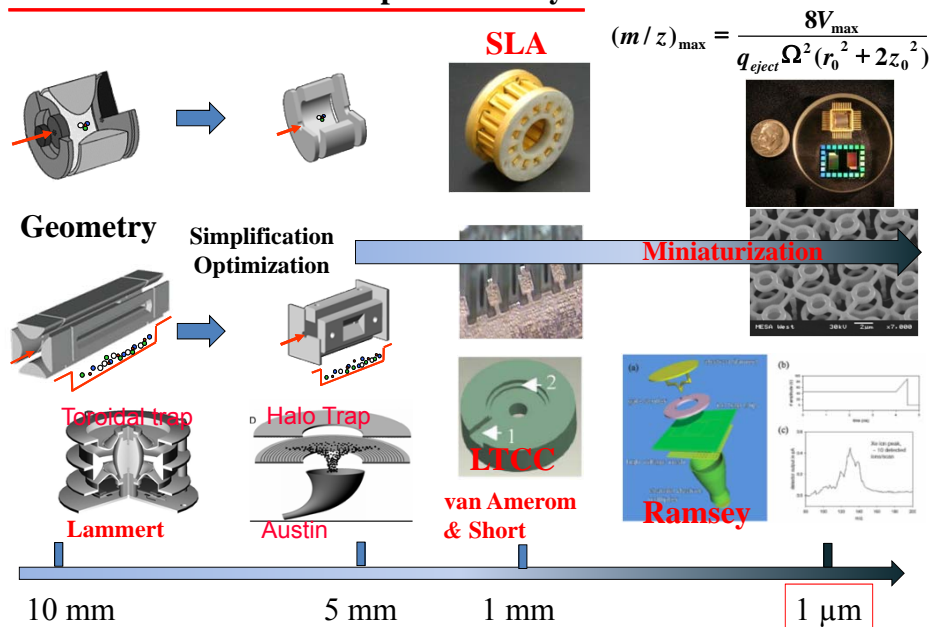


## Micro-fabricated Mass Analyzer

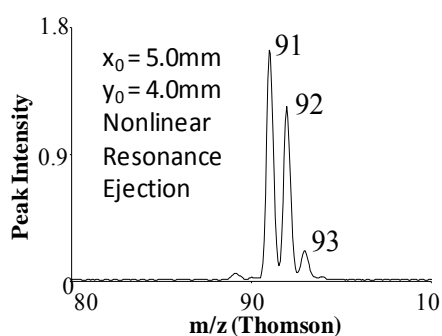
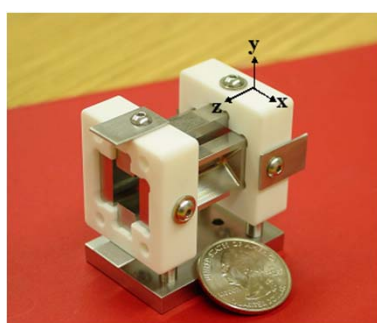
Syms, Imerial  
V-Groov Filter



**Miniaturization of Ion Trap Mass Analyzer**

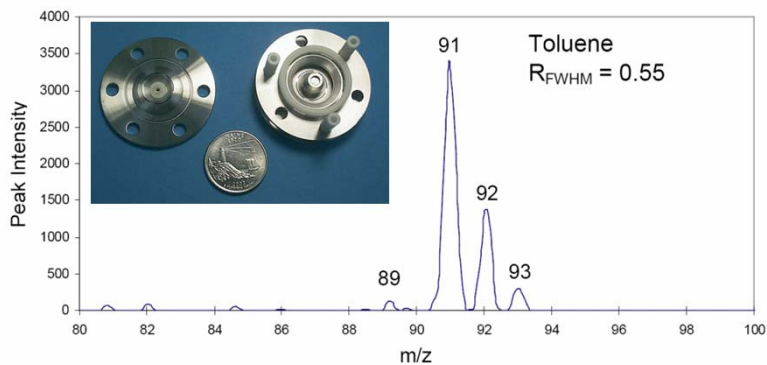


**Rectilinear Ion Trap**

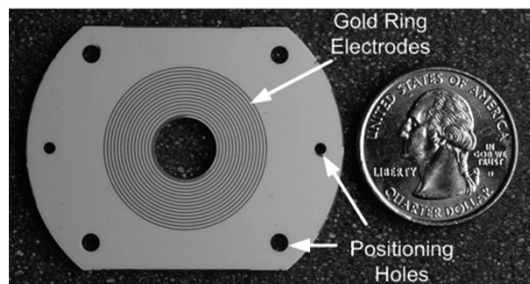
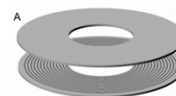
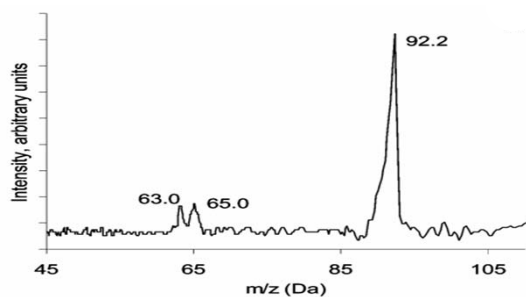




### Toroidal Ion Trap



### Halo Trap



## Tradeoff and Balance

Low Scan Voltage -  $V_{RF}$  vs.  $D$ - Deep Trapping Potential Well

$$V_{RF} \propto \frac{m}{z} * r^2 * \Omega_{RF}^2$$

$$D \propto V_{RF}$$

$r$ :  $r_0$ , for 3D or  
 $x_0$ , for 2D linear

$\Omega_{RF}$ : RF frequency

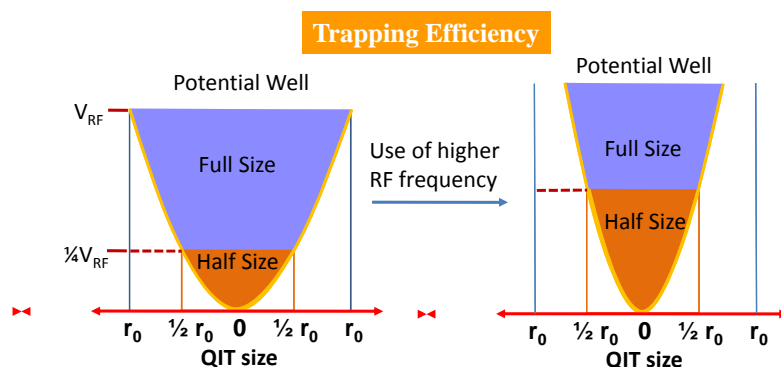


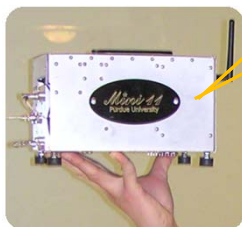
Figure 7

## Impact of Trap Size

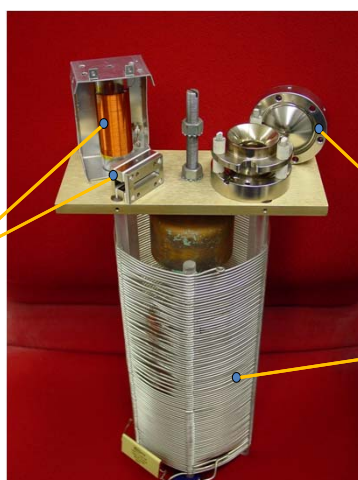
RF Voltage and Power?

$$(m/z)_{\max} = \frac{8V_{\max}}{q_{\text{eject}} \Omega^2 (r_0^2 + 2z_0^2)}$$

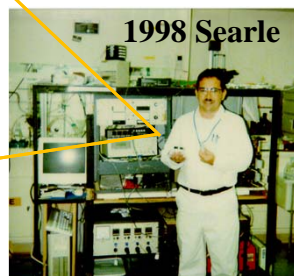
**Mini 11**  
 5mm 2D trap  
 Unit Resolution  
 Mass range:  $m/z$  800



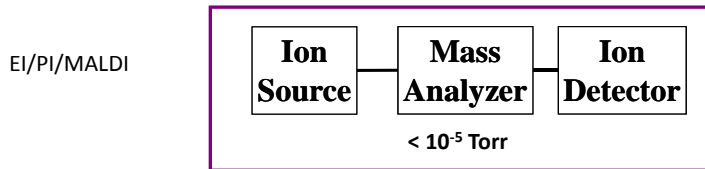
2007



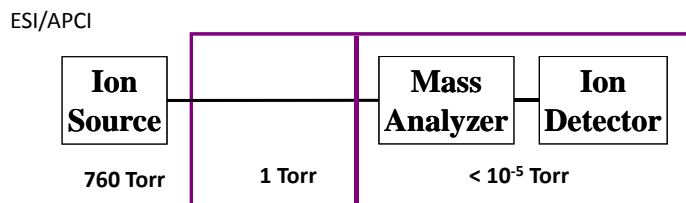
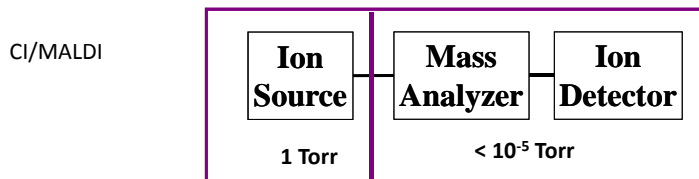
**ITMS**  
 10mm 3D trap  
 Unit Resolution  
 Mass range:  $m/z$  700



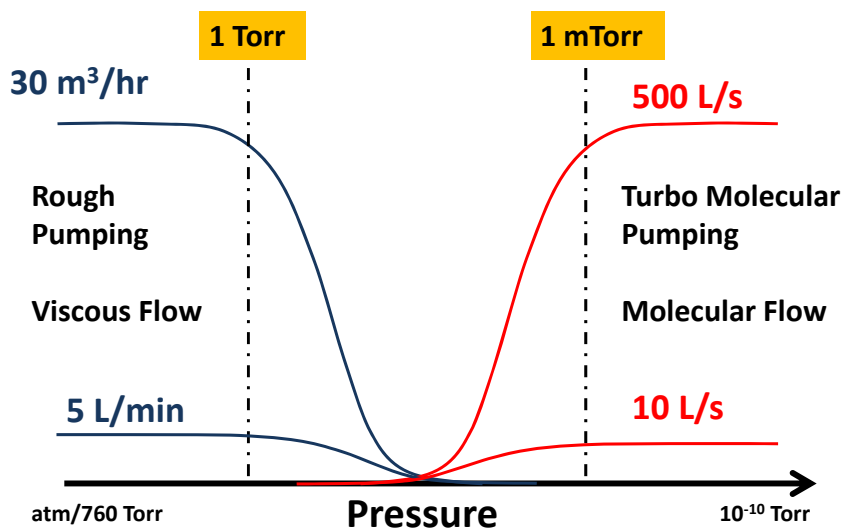
Pressure matching between the ion source and the mass analyzer



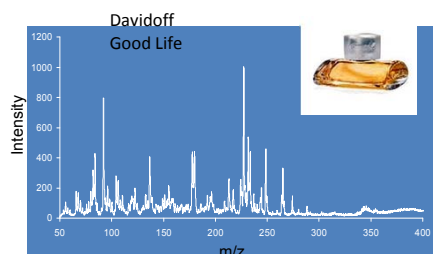
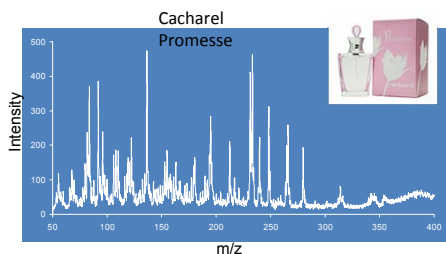
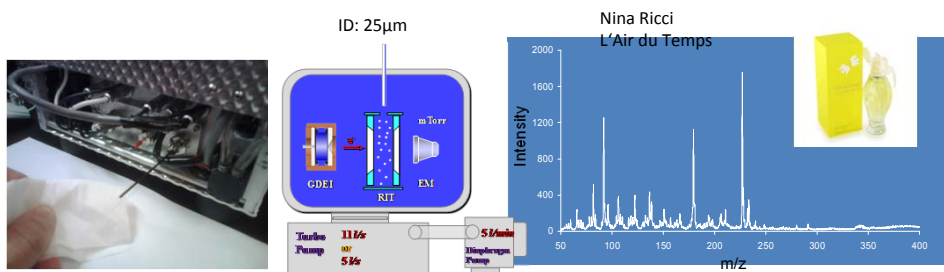
Differential pumping



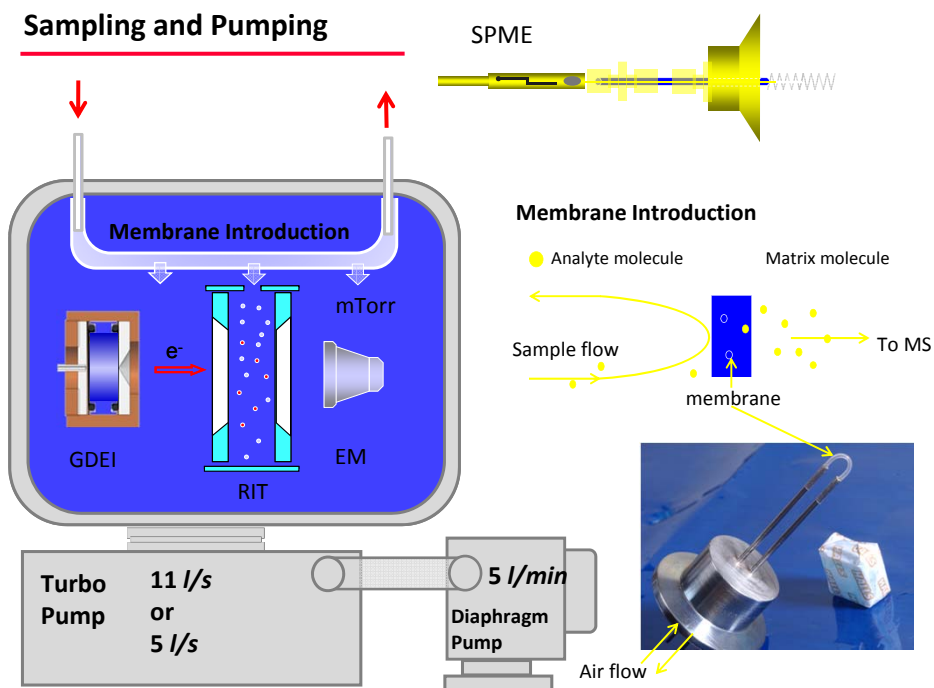
Pumping



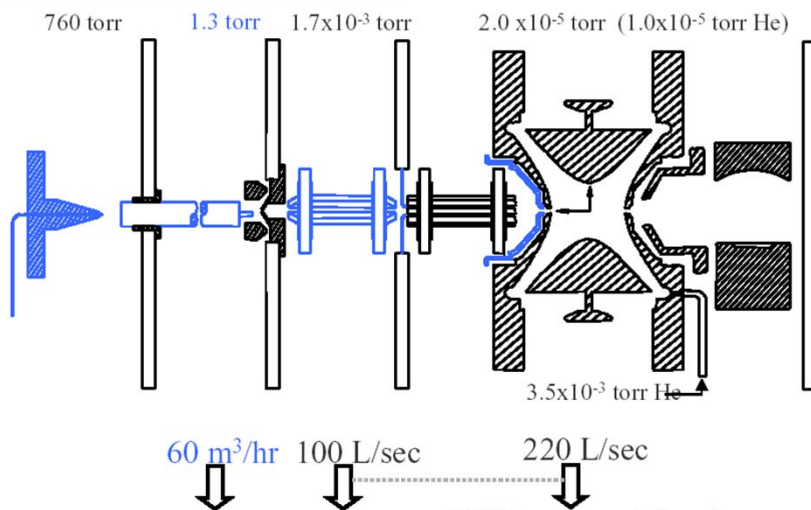
Direct Leak



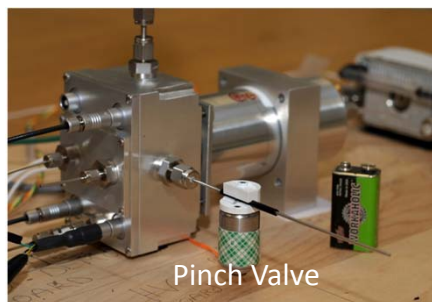
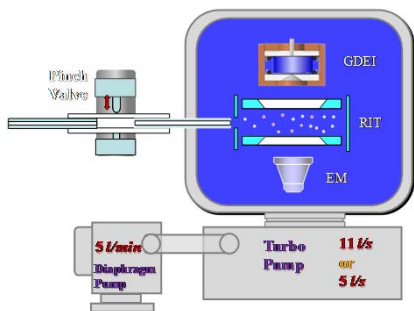
Sampling and Pumping



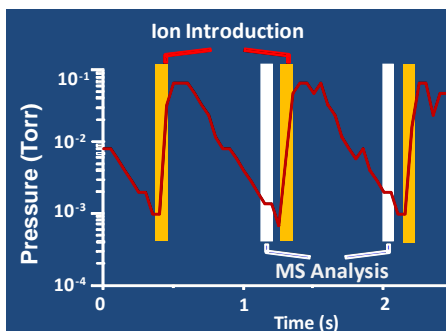
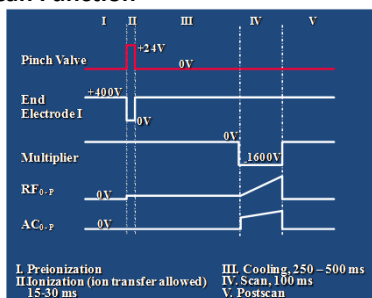
### Gas and Ions



### Discontinuous Atmospheric Pressure Interface (DAPI)



### Scan Function



		Self-Sustainable Portable Systems							Portable Systems without Rough Pumping			
		Mini 10/Mini 11 (3, 4)	ChemCube (119)	Guardion-7 (5)	Suitcase TOF (9)	Griffin 600 (120)	Ion-Camera (121)	Palm-Portable MS (52)	HAPSITE (75)			
Developer		Purdue University	Microsaic Systems	Torion Technologies	Johns Hopkins Applied Physics Lab	Griffin Analytical	O-I-Analytical	Sam Yang Chemical	Inficon			
Weight		10 kg /4 kg	14 kg	11 kg	N/A	15 kg	18 kg	1.5 kg	18 kg			
power		70 W/30w	50 W	75 W	N/A	N/A	75 W	5 W	< 150 W			
Mass Analyzer		Rectilinear ion trap	Quadruple mass filter	Toroidal ion trap	Time of flight	Cylindrical ion trap	Mattauch-Herzog sector	Cylindrical ion trap	Quadrupole mass filter			
MS/MS		Yes	No	Yes	No	Yes	No	No	No			
Sampling /Ionization		MIMS, direct leak, GDEL, APCL, ESI, DESI, LTP	SPME EI	SPME, Mini GC EI	MALDI	SPME, MIMS EI	Direct gas leak EI	Pulsed gas leak EI	GC EI			
Mass range /Resolution		m/z 550, R= 550; m/z 2000, R = 100	m/z 400, R = 100	m/z 500, R = 500	m/z 70,000, R = 70	m/z 425, R = 400	m/z 300, R=300	m/z 300, R = 150	m/z 300, R = 300			
System Photo												